AD-A111 362 OHIO STATE UNIV COLUMBUS ELECTROSCIENCE LAB F/G 17/9
THE PROPAGATION OF ELECTROMAGNETIC VIDEO PULSES WITH APPLICATIO--ETC(U)
DEC 76 G A BURRELL, L PETERS, A J TERZUOLI DAAG53-76-C-0179
UNCLASSIFIED ESL-4460-2 NL

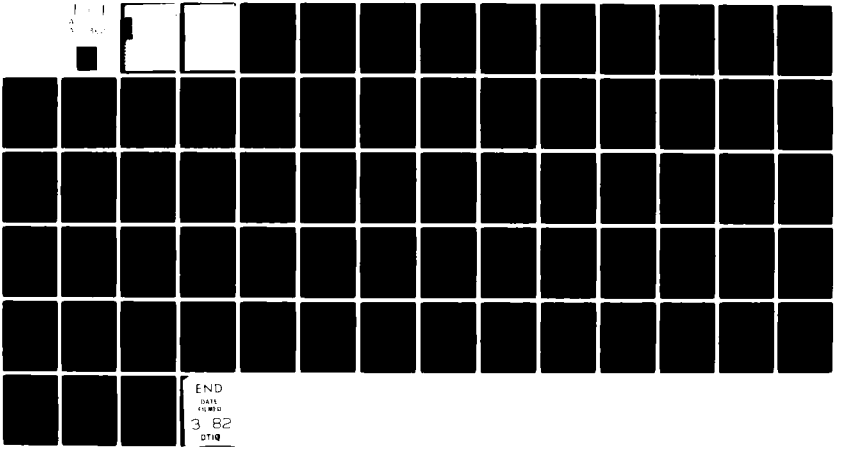

END
DATE FILMED
3 82
DTIC

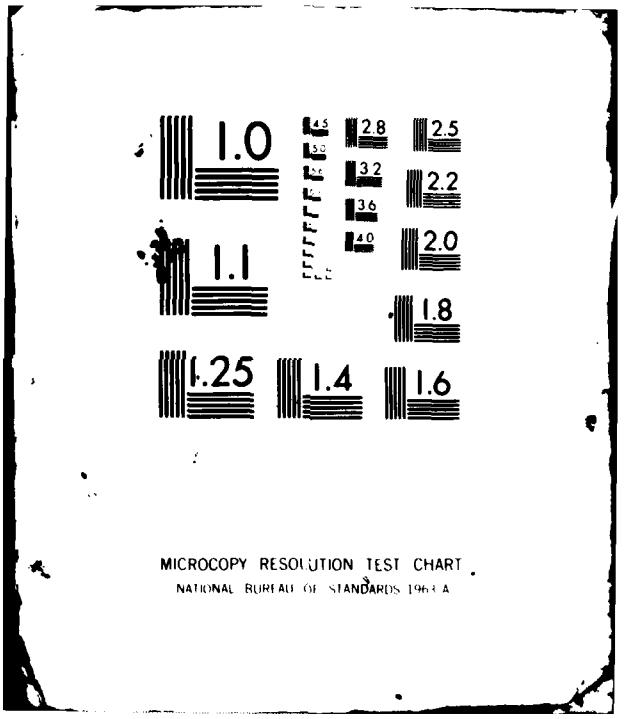
1.0
1.1
1.25
1.4
1.6
1.8
2.0
2.2
2.5
2.8
3.2
3.6
4.0
MICROCOPY RESOLUTION TEST CHART
NATIONAL BUREAU OF STANDARDS 1963 A

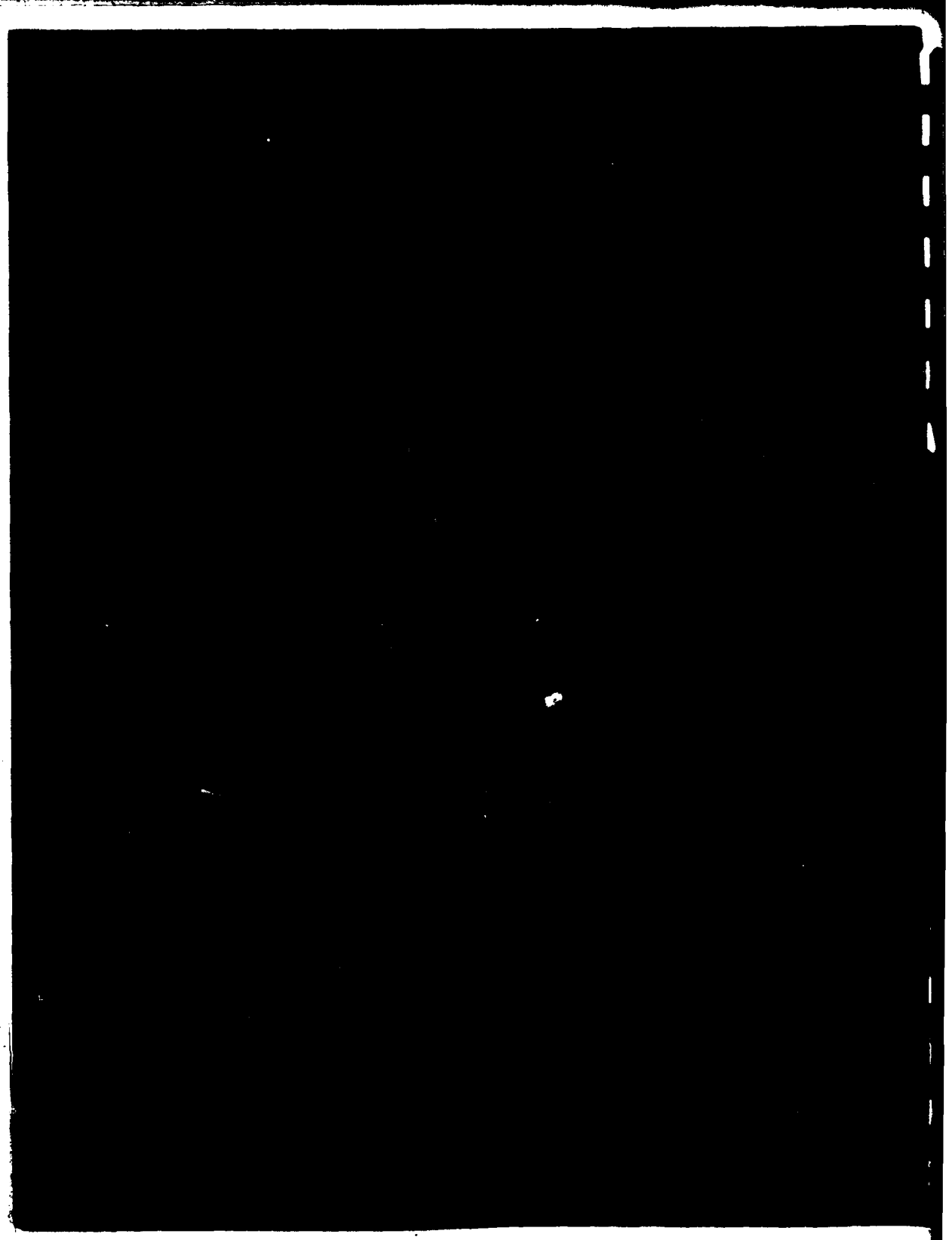

UNCLASSIFIED

SECURITY CLASSIFICATION OF THIS PAGE (When Data Entered)

REPORT DOCUMENTATION PAGE		READ INSTRUCTIONS BEFORE COMPLETING FORM
1 REPORT NUMBER	2. GOVT ACCESSION NO. AD-A044362	3 RECIPIENT'S CATALOG NUMBER
4 TITLE (and Subtitle) THE PROPAGATION OF ELECTROMAGNETIC VIDEO PULSES WITH APPLICATION TO SUBSURFACE RADAR FOR TUNNEL DETECTION		5 TYPE OF REPORT & PERIOD COVERED Technical Report
		6. PERFORMING ORG. REPORT NUMBER ESL 4460-2
7 AUTHOR(s) G. A. Burrell L. Peters, Jr. A. J. Terzuoli, Jr.		8. CONTRACT OR GRANT NUMBER(s) Contract DAAG53-76-C-0179
9 PERFORMING ORGANIZATION NAME AND ADDRESS The Ohio State University ElectroScience Laboratory, Department of Electrical Engineering, Columbus, Ohio 43212		10 PROGRAM ELEMENT PROJECT TASK AREA & WORK UNIT NUMBERS
11 CONTROLLING OFFICE NAME AND ADDRESS Department of the Army US Army Mobility Equipment Research & Development Command, Ft. Belvoir, Va 22060		12 REPORT DATE December 1976
		13 NUMBER OF PAGES 66
14 MONITORING AGENCY NAME & ADDRESS(if different from Controlling Office)		15 SECURITY CLASS. (of this report) Unclassified
		15a DECLASSIFICATION DOWNGRADING SCHEDULE

16 DISTRIBUTION STATEMENT (of this Report)

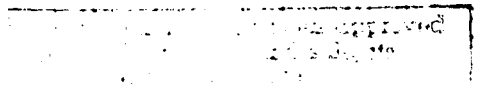

17 DISTRIBUTION STATEMENT (of the abstract entered in Block 20, if different from Report)

18 SUPPLEMENTARY NOTES

19 KEY WORDS (Continue on reverse side if necessary and identify by block number)

Underground radar	High frequency window	Impedance
Numerical results	Tunnel detection	
Propagation	Lossy media	
Videopulse radar	Dipole	
Low frequency window	Conducting media	

20 ABSTRACT (Continue on reverse side if necessary and identify by block number)

Pulse propagation in lossy media is considered over a seven decade frequency band to 1 GHz with a view to determining the design principles of video pulse subsurface radar systems. Two different radars may be required depending upon whether signal propagation is within the Low Frequency Window (LFW) or the High Frequency Window (HFW) as defined by Gabillard et al. (1971). The antenna type chosen is a finite length dipole. In the LFW it is essential that the dipole be maintained in conducting contact

DD FORM 1 JAN 73 1473 EDITION OF 1 NOV 65 IS OBSOLETE

UNCLASSIFIED

SECURITY CLASSIFICATION OF THIS PAGE (When Data Entered)

20.

with the ground whereas in the HFW the antenna may be insulated. An LFW radar operates in a frequency range which is too low to excite resonances of subsurface targets whose characteristic dimensions are of the order of 1-2 meters (tunnels): consequently LFW radars are potential detectors of such targets. An HFW radar can operate in frequency bands that includes target resonances for the 1-2 meter radius tunnels. Consequently HFW radars are potential identifiers of targets, although LFW radars can be operated in a mapping mode for identification purposes. The choice of an LFW or an HFW radar depends upon the depth of operation and the constitutive parameters of the ground. A design chart is presented for the appropriate selection of the radar type. Attenuation curves describing the signal loss for both LFW and HFW radars are also presented.

TABLE OF CONTENTS

INTRODUCTION

It is interesting to note that one of the first video pulse radar systems was proposed in 1937 by Melton (1937). However, the first practical video pulse radar system introduced for tunnel detection was the Geodar system (Lerner, 1974). There have been many research organizations involved in this type of system. Some of these are MIT, SRI, SWRI, Calspan, Teledyne, and GSS.

The work at the ElectroScience Laboratory has followed three directions. One of these is the development of a pipe detector system under the guidance of Dr. J. Young and patented by Young and Caldecott (1976). This has resulted in a unit which is to be marketed by Microwave Associates Inc. under the trade name of Terrascan. Dr. Moffatt had earlier used a somewhat less sophisticated system to detect a variety of geological structures (Moffatt et al (1973)). These systems have two major improvements over the Geodar unit. The most important advance is an improved loaded crossed dipole antenna system. This development eliminated the hybrid T-R and ATR system used in the Geodar unit to isolate the received and transmitted pulses. The second advantage is that this antenna system can be made insensitive to reflections from planar parallel surfaces. This greatly reduces the clutter in any subsurface radar, and such a system is ideal for observing any scatterers, such as tunnels, that are symmetric with respect to the antenna axis.

More recently Burrell and Peters (1976) conducted a study on the applicability of this type of radar system for deep penetration (depths of the order of a kilometer). It has been found that such systems appear to be practical but very careful system design is necessary. For deep penetration, it is found this radar must operate within the low frequency window as defined by Gabbilard et al (1971). This also implies that the antenna must be in electrical contact with the conducting ground. This offers several significant advantages. First, the propagation in the medium when the frequency of transmission is within the LFW is independent of conductivity and frequency when a voltage pulse is applied to the antenna terminals. Second, the antenna impedance, to a good approximation, is frequency independent and is a constant resistance which is easily matched to a well designed pulser. Thus a pulse can be transmitted through the lossy medium without distortion.

The goal of this report is to extend this work to address the problem of detection and identification of targets to a depth of 120 m. In particular, this report considers pulse propagation in lossy media with particular emphasis on its application to subsurface video pulse radar with ranges up to 120 m. Signal radiation from a current element in a lossy medium is studied and two possible frequency bands of operation are identified. These are the Low Frequency Window (LFW) and High Frequency Window (HFW) as defined by Gabillard et al,(1971). Propagation in each window is considered separately. A suitable antenna type for subsurface

radar has been chosen, but detailed antenna design is not covered in this report which addresses propagation loss and signal distortion. Nevertheless antenna design is an important facet of subsurface radar, and modified antenna designs will slightly affect the attenuation constants presented in this report (the effect is expected to be of the order of 2-3 dB).

In Section 1 the propagation constant for plane waves in a lossy medium is plotted for use as a design aid in the later sections. Section 2 examines the fields of a current element as functions of frequency, range and ground parameters. A physical picture of the mechanism of radiation from the current element is presented to explain the shapes of the curves. Section 3 presents generalized curves for the E field of the current element and introduces the LFW and HFW concepts. This follows Gabillard et al (1971). A design chart is presented which can be used to determine whether an LFW or an HFW radar is required for a particular application (determined by the ground constitutive parameters and the radar range). Section 4 investigates the desired properties of an antenna for subsurface radar, and concludes that the dipole is a most suitable antenna type for the application. In Section 5 the fields of finite length dipoles are considered and their relation to the fields of a current element established. In particular it is found that the fields of a current element (which are simply evaluated) are a reliable guide to the type of radar (LFW or HFW) required.

A computer model to study the propagation characteristics of the system comprising the antenna(s) and the medium is developed in Section 6. This model is then used to determine design data for LFW radars (Section 7) and HFW radars (Section 8). A brief summary of how to use this design data is given in Section 9. It is noted that the frequency band of operation of an LFW radar is generally too low to get information about the resonances of targets as electrically small as 1 meter radius tunnels. Consequently LFW radars are potential detectors of such targets. HFW radars can operate at frequencies of hundreds of MHz, and can be regarded as potential identifiers of such targets.

A good understanding of the physical mechanisms involved is essential to the understanding of any subject. Many of the characteristics of antennas and propagation in lossy media do not follow intuitively from the familiar characteristics in free space. Consequently those concepts presented in this report which are "foreign", or differ from those which occur in free space situations, are expanded in some detail and often from more than one point of view. This is done to help the reader to thoroughly understand the concepts presented.

1. THE ATTENUATION CONSTANT FOR PLANE WAVES PROPAGATING IN A LOSSY MEDIUM

The propagation constant γ for a lossy medium having a conductivity σ mhos/m and a relative permittivity (dielectric constant) ε_r is given by

$$\gamma = [j\omega\mu(\sigma+j\omega\varepsilon)]^{1/2} = \alpha+j\beta \qquad (1)$$

where ω is the radian frequency ($2\pi f$), and $\varepsilon=\varepsilon_0\varepsilon_r$ is the permittivity, ε_0 is the permittivity of free space, α is the attenuation factor and β is the phase constant. These are given by

$$\alpha = \omega\sqrt{\frac{\mu\varepsilon}{2}\left(\sqrt{1+\frac{\sigma^2}{\omega^2\varepsilon^2}}-1\right)} \tag{2}$$

$$\beta = \omega\sqrt{\frac{\mu\varepsilon}{2}\left(\sqrt{1+\frac{\sigma^2}{\omega^2\varepsilon^2}}+1\right)} \tag{3}$$

The low frequency approximations for α and β are

$$\alpha = \sqrt{\frac{\omega\mu\sigma}{2}} \tag{4}$$

$$\beta = \sqrt{\frac{\omega\mu\sigma}{2}} \tag{5}$$

and the high frequency approximations are

$$\alpha = \frac{\sigma}{2}\sqrt{\frac{\mu}{\varepsilon}} \tag{6}$$

$$\beta = \omega\sqrt{\mu\varepsilon} \tag{7}$$

Note that (4) and (5) are independent of ε and (6) is independent of frequency.

The attenuation of plane monochromatic waves propagating through a lossy medium depends upon α. Figure 1 shows α in decibels/meter for lossy media with constitutive parameters spanning a range typical of the ground likely to be encountered in this study. Note that when $f<100$ KHz, α is given by (4). The high frequency form (6) is valid for frequencies greater than 2 MHz for $\sigma=.001$ mhos/m and $\varepsilon_r=4$, but is not valid until 100 MHz when $\sigma=.02$ mhos/m and $\varepsilon_r=16$.

For pulse signals, the attenuation depends upon the value of α over the frequency range for which the pulse signal has significant energy. For propagation at high frequencies $\partial\beta/\partial\omega$ = constant = 1/phase velocity and consequently the shape of a transmitted waveform is preserved as long as its spectral components lie in the appropriate frequency band. For propagation at low frequencies, the shape of the transient waveform is preserved primarily because the products $\alpha L = \beta L$ are negligible (L = path length in the medium).

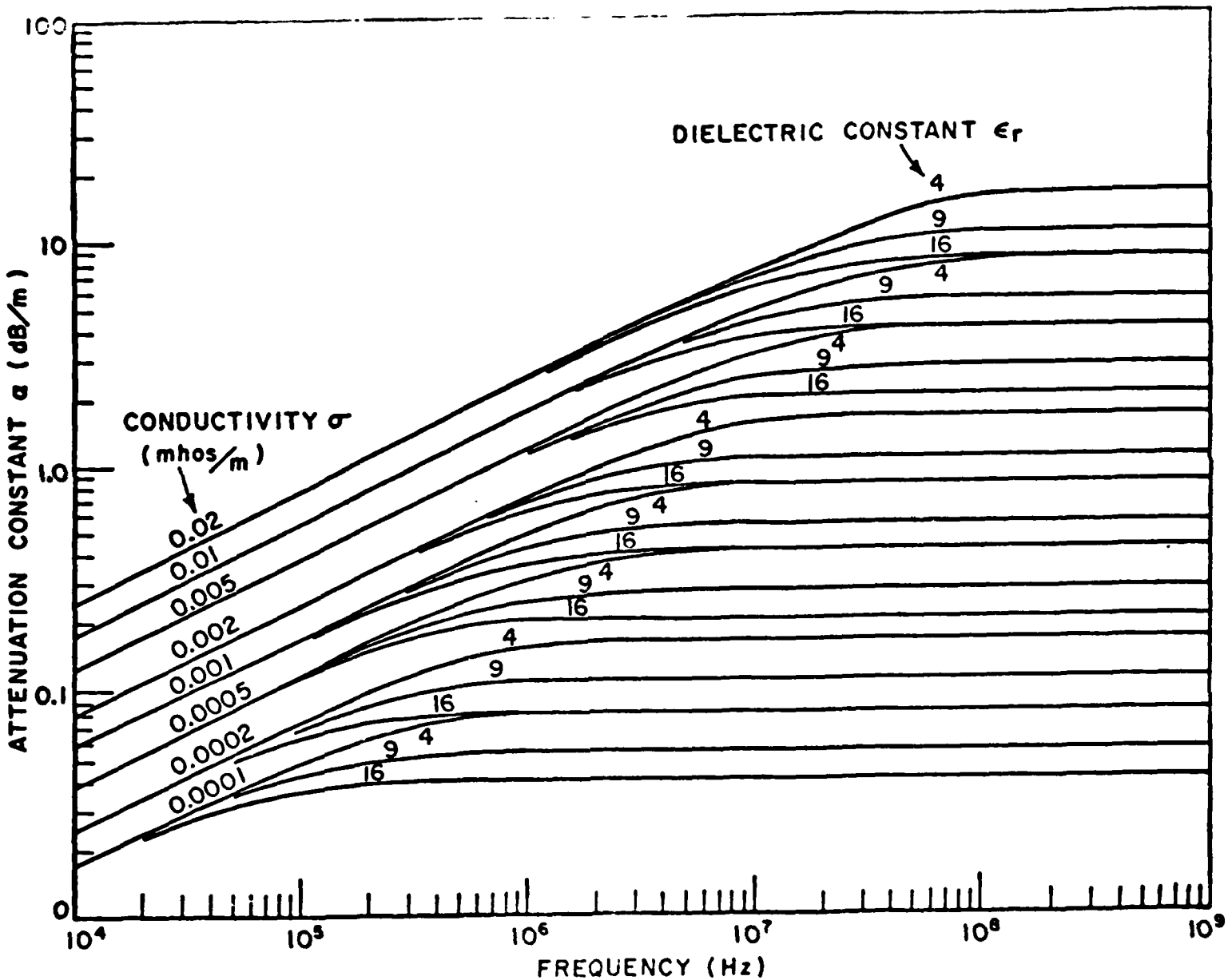

Figure 1. Attenuation constant α plotted as a function of frequency for lossy media.

2. THE ELECTRIC FIELD INTENSITY OF A CURRENT ELEMENT IN A LOSSY MEDIUM

The attenuation factor α applies to the propagation of plane waves through a lossy medium. A better idea of the transmission by a practical antenna system into a lossy medium can be obtained by examining the fields of an elementary dipole.

The electric field a distance r from an infinitesimal electric dipole is given by Schelkunoff and Friis (1952, p. 119):

$$E_\theta = \frac{Id\ell \sin\theta}{4\pi(\sigma+j\omega\varepsilon)r^3} (1 + \gamma r + \gamma^2 r^2)e^{-\gamma r} \tag{8}$$

In (8), I is the current which is constant along the length $d\ell$ of the element, and θ is the elevation angle of the conventional spherical coordinate system. The dipole is coincident with the z axis. The behavior of E_θ as the frequency changes is facilitated by manipulating (8) in the following way (Gabillard et al. 1971). For zero frequency, (8) becomes

$$E_{\theta_o} = \frac{I_o d\ell \sin\theta}{4\pi\sigma\, r^3} \tag{9}$$

Divide (9) into (8) to obtain

$$e_\theta = \frac{\sigma}{\sigma+j\omega\varepsilon} (1+\gamma r+\gamma^2 r^2)e^{-\gamma r} \tag{10}$$

Equation (10) is the ratio of the electromagnetic field component E_θ at the radian frequency ω to the same component for zero frequency. The variation of the electric field with σ,ε and f is described by this equation (Gabillard et al 1971).

Figures 2-4 show (10) plotted over seven decades of frequency for a range of conductivities and dielectric constants. The important feature in these plots is that when the range and conductivity are low, and ε_r is high, $|e_\theta|$ is constant at low frequencies and increases smoothly at high frequencies. When the range and conductivity are both high, $|e_\theta|$ rises to a peak of 1.45 (3.23 dB), then attenuates sharply as the frequency increases. This means that at high frequencies there is effectively no deep penetration of electromagnetic waves from a current element into a highly conducting medium. Notice that for certain combinations of conductivity and range between the two extremes there is a small dip in the frequency response, but high frequency transmission is possible.

It is worth examining (10) in some depth to determine the reason for the shape of the frequency responses displayed in Figures 2-4 Basically it is the interference between the three terms in (10) and the

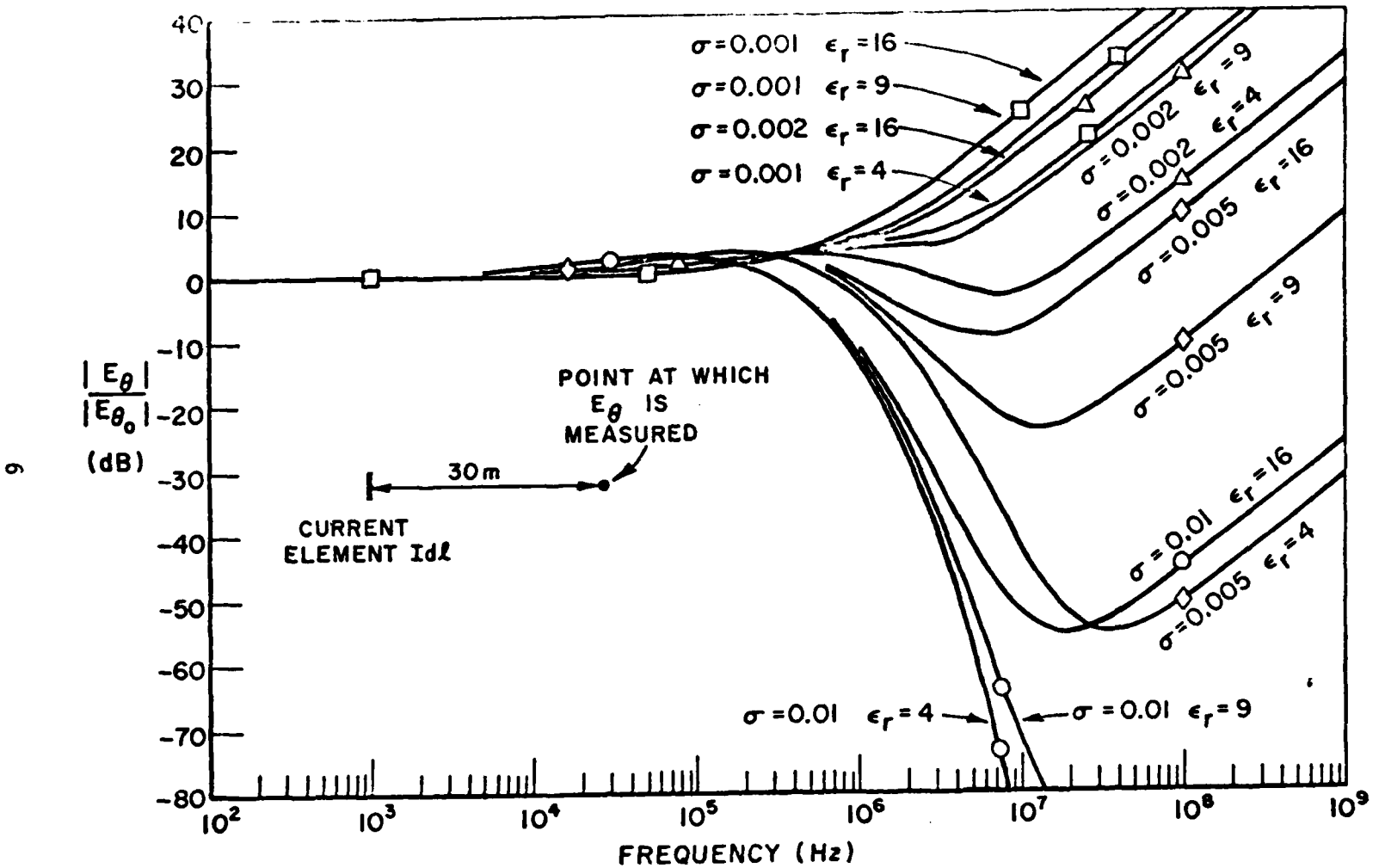

Figure 2. Normalized electric field strength 30 m from current element for lossy media.

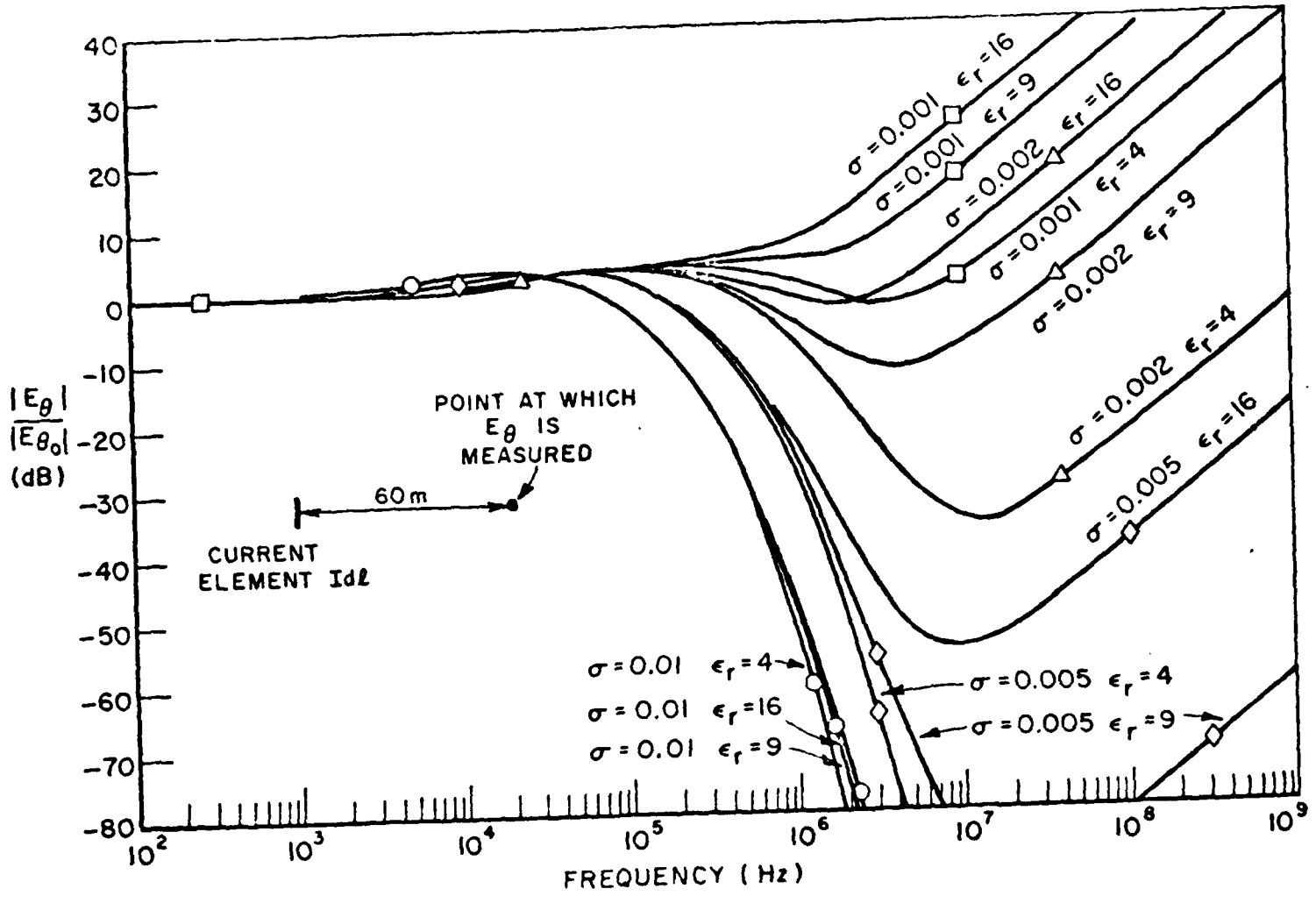

Figure 3. Normalized electric field strength 60 m from current element for lossy media.

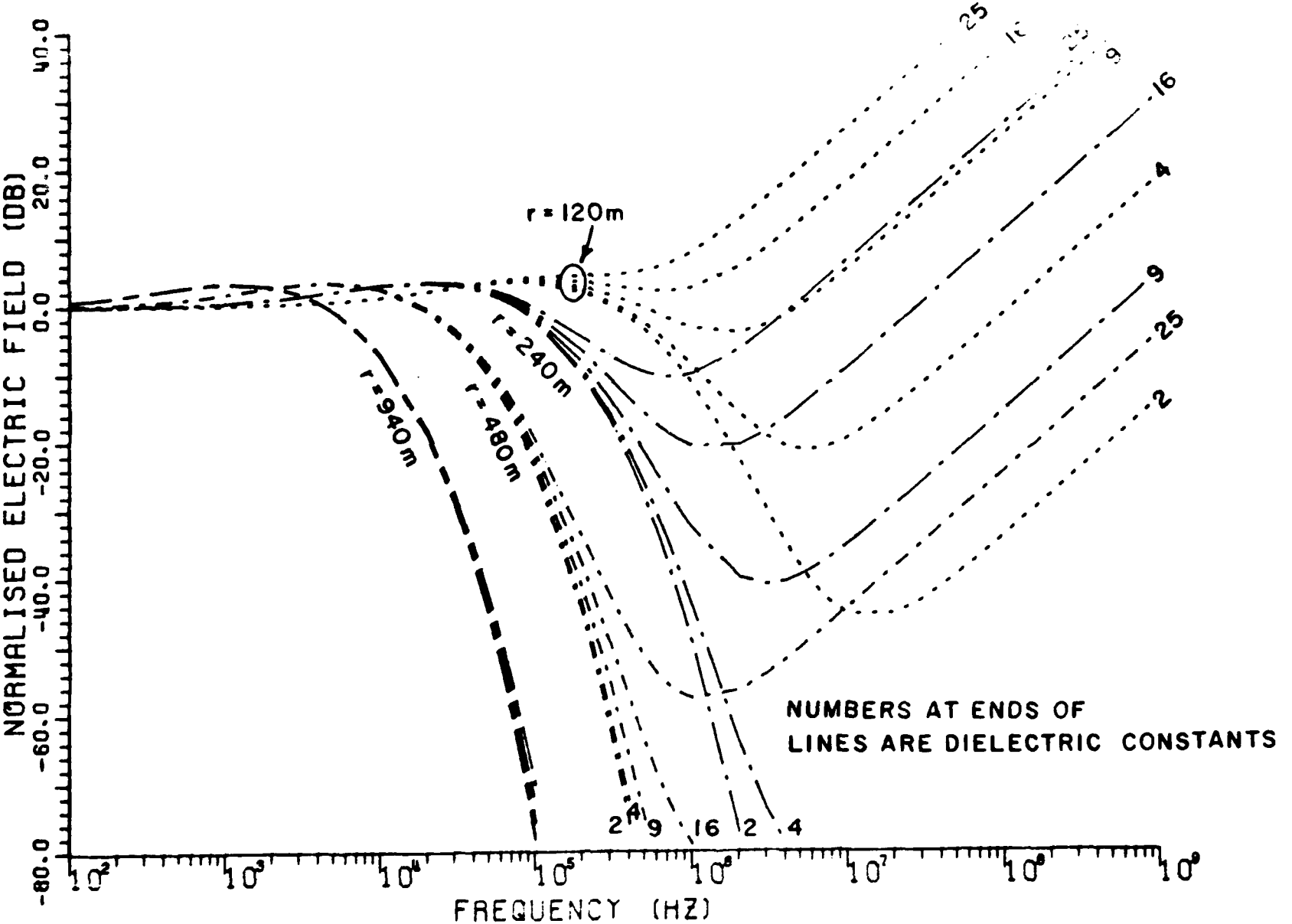

Figure 4. Normalized electric field broadside to current element for media of conductivity σ=.001 mhos/m. Results are presented for different ranges.

behavior of γ with frequency which change the shape of the frequency response. When the range and the frequency are both small the dominant term in (10) is the first term inside the brackets (which is the electrostatic field term). Hence $|e_\theta|$ is approximately unity. As the frequency increases (thereby increasing γ) the second and third terms in the brackets in (10), grow in amplitude and $|e_\theta|$ rises in amplitude to a maximum of 3.23 dB. This peak occurs when $\gamma r \approx 2.5$. As the frequency increases still further the radiation field (the last term inside the brackets) dominates the expression contained within the brackets. However, an increase in frequency also increases the attenuation introduced by the $e^{-\alpha r}$ factor in $e^{-\gamma r}$. This attenuates the signal as the frequency increases because α increases as $\sqrt{f}$ (see (4)), i.e., the decrease due to the exponential terms becomes greater than the increase due to the $(\gamma r)^2$ term. The net effect is that a severe attenuation of the fields occurs when the conductivity (and hence α and $e^{-\alpha r}$) is large and r is large. However when the conductivity is low, α reaches its high frequency form (which is constant, see (6)) before severe attenuation of the fields occurs. Consequently the frequency response displays at most a small dip. Notice that in Figures 2-4 $|e_\theta|$ begins increasing when the frequency is high enough so that α becomes constant (the high frequency form), as shown in Figure 1. Hence $e^{-\gamma r}$ only introduces a constant attenuation which is independent of frequency, and $|e_\theta|$ is proportional to frequency. This explains the 6 dB/octave of frequency increase in $|e_\theta|$ at high frequencies.

Finally, it is observed that deeper penetration without dispersion occurs for the dipole radiated fields at higher values of γr than is the case for plane wave propagation primarily because of the effect of the $(\gamma r)^2$ term in Equation (10).

3. THE HIGH FREQUENCY AND LOW FREQUENCY WINDOWS

Gabillard et al (1971) have reduced the curves shown in Figures 2-4 to a set of universal curves, and have defined a Low Frequency Window (LFW) and a High Frequency Window (HFW). Gabillard et al's curves are shown in Figure 5. The LFW is defined as that band of frequencies from zero frequency to a cutoff frequency f_m, which is the frequency at which $|e_\theta|$ falls to -3 dB. It is given by

$$f_m = \frac{3.76 \times 10^6}{r^2 \sigma} \tag{11}$$

where r is the distance to the observation point in meters, and σ is in mhos/meter.

The HFW is defined as that band of frequencies from f_M, which is the frequency at which $|e_\theta|$ again becomes greater than 1, to infinity. Notice that for some ground parameters and ranges, e.g., when σ=.001, ε_r=16 and r=30 m, $f_M < f_m$, so that there is no dip in the frequency response. Notice also that for more lossy ground (e.g., σ=.01 mhos/m, ε_r=4) f_M is so high

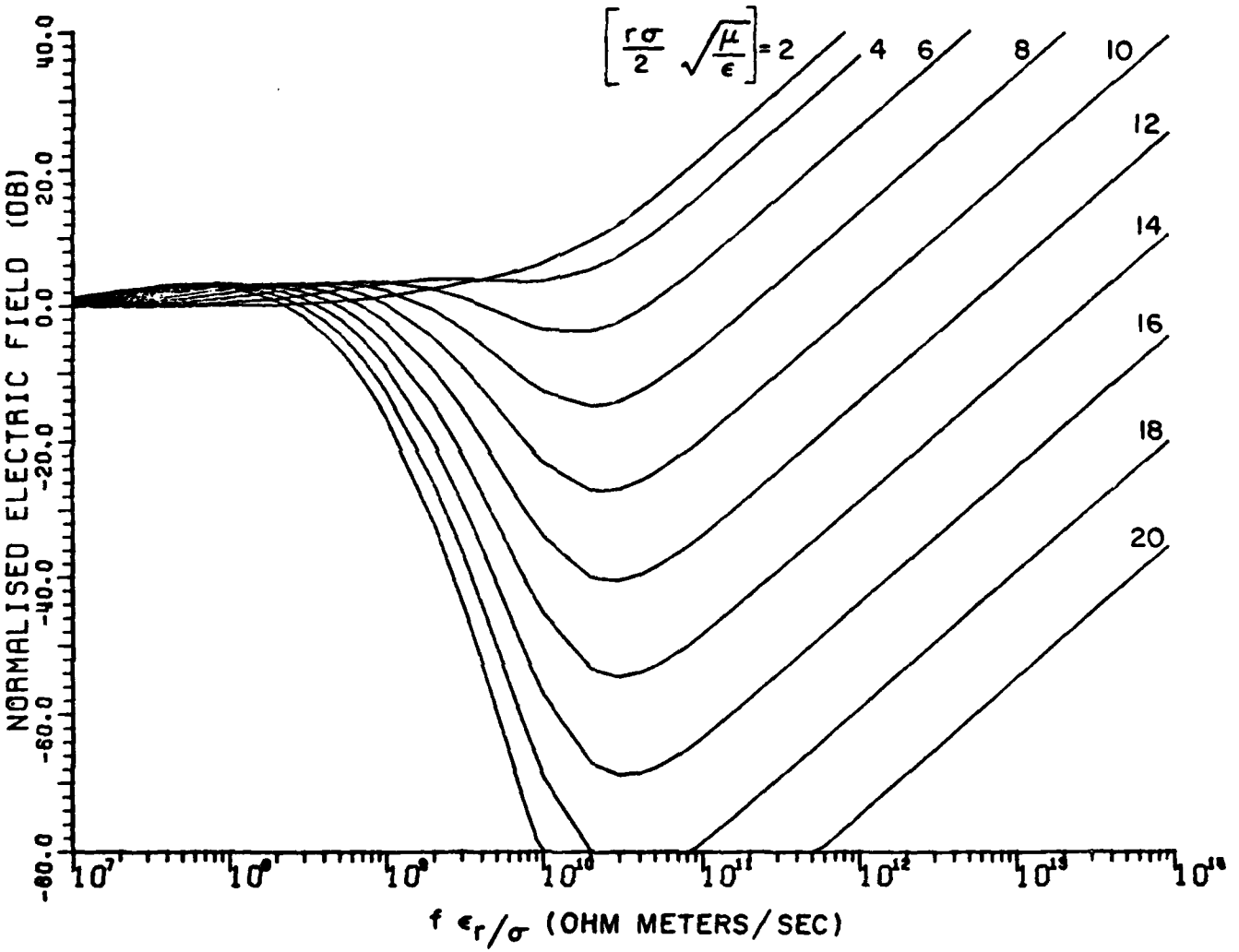

Figure 5. Universal curves for the normalized electric field of a current element in lossy media (due to Gabillard et al, 1971)

that practical pulse signal sources could not be used (we have limited our calculations to 1 GHz since high amplitude pulse generators with significant energy beyond 1 GHz are uncommon).

Inspection of Figures 2-5 indicate that it is practical to use the HFW providing the dip in the frequency response is not excessive. We have set an arbitrary limit of about -10 dB on the amplitude of the dip if operation in the HFW is to be possible. When the dip is greater than this, $|e_0|$ does not again exceed unity until the frequency is beyond the range of many practical pulse generators. This condition is met when the radar range is less than $4L_c$, where L_c is the characteristic length of the medium (Gabillard et al, 1971) and is given by

$$L_c = \frac{2}{\sigma}\sqrt{\frac{\varepsilon}{\mu}} \tag{12}$$

Hence our arbitrary design condition is that for operation of an underground radar to be possible in the HFW, then

$$d < \frac{8}{\sigma}\sqrt{\frac{\varepsilon}{\mu}} \tag{13}$$

Note that in deducing the condition $d<4L_c$, the radar range d is half the total propagation distance r. It is important to remember that r=2d when using (11) to determine the LFW cutoff frequency for a particular radar.

Figure 6 presents (13) in graphical form. As an example, consider a radar design for which the ground constants are σ=.001 mhos/m and ε_r=4. The point on the graph defining this medium lies to the left of the d=30 m line. This means that the HFW can be used for a radar which has a maximum range of 30 m (≈100 ft). However the same point lies to the right of the d=60 m line. This means that for a radar which is to operate to depths of 60 m and greater, the operating bandwidth of the radar is restricted to the LFW, whose cutoff frequency is given by (11). It should be remembered that Figure 6 is based on an arbitrary criterion which is the allowable depth of a null in the elementary dipole frequency response, but it turns out that the depth of the null is very sensitive to the range and ground constitutive parameters, so that in practice Figure 6 gives reliable data. When the point defining the ground parameters lies very close to the line for the desired range, Equation (10) should be plotted and f_M compared with the spectra of the available pulse sources and the frequency range for which data is required before a decision is made.

The design of the radar depends upon the frequency range. In the LFW, propagation is largely due to conduction currents. This means that good electrical contact between the transmitting and receiving antennas and the ground is essential. However in the HFW propagation is due to the displacement currents (Gabillard et al, 1971) and it turns out that electrical contact with the ground is not essential. Consequently

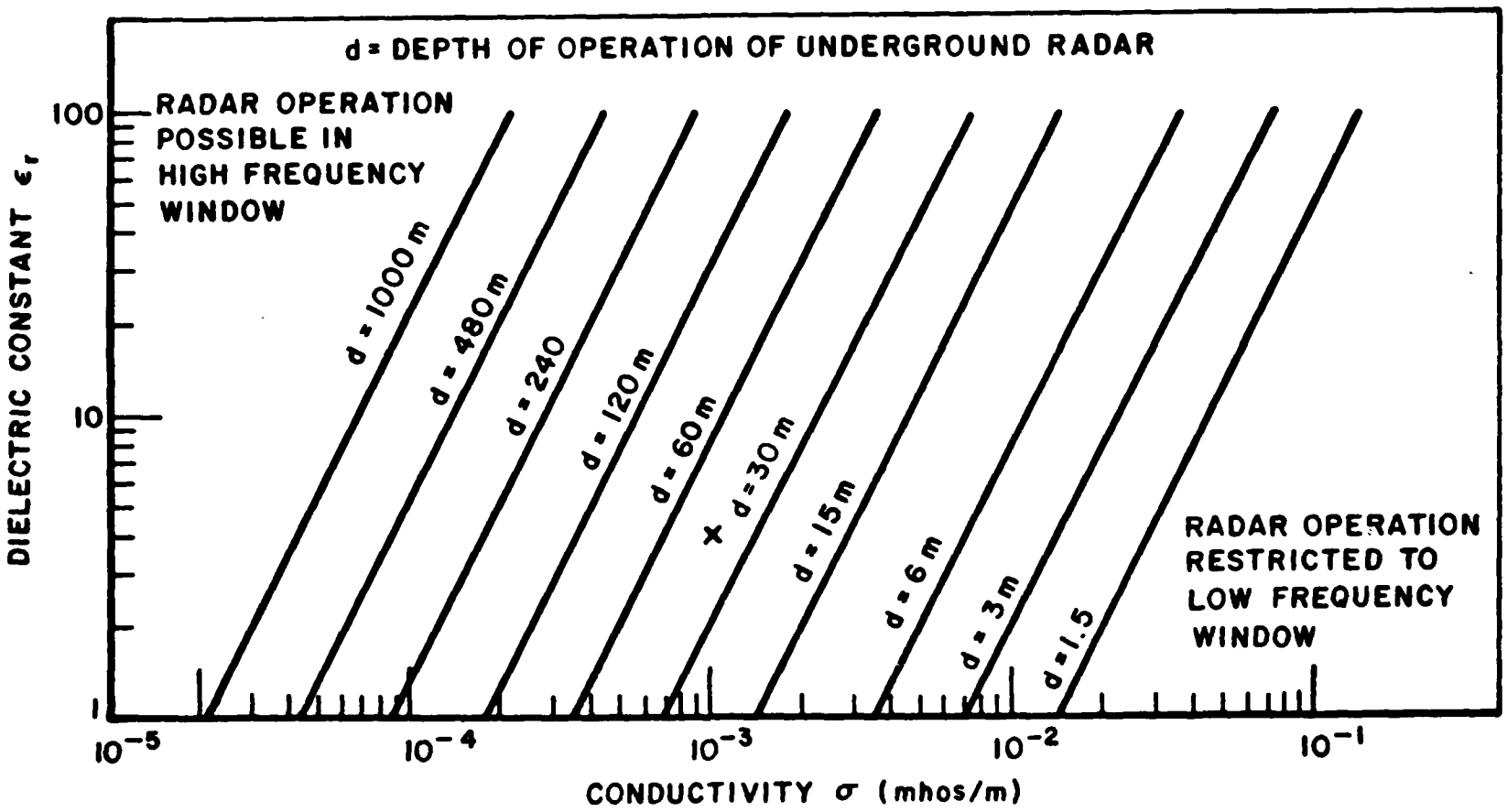

Figure 6. Design graph to determine whether radar operation should be in HFW or LFW.

a radar designed to operate in the HFW can have an antenna which is merely close to the ground. For a LFW radar however, particular care needs to be taken to ensure that the antenna is in electrical contact with the ground. This is based on the fact that the input impedance of the insulated antenna is a constant resistance. This means that whereas the HFW radar can be operated as a mobile system, the LFW radar cannot.

4. THE CHOICE OF AN ANTENNA TYPE FOR AN UNDERGROUND ELECTROMAGNETIC RADAR

The primary requirement of an antenna for a subterranean radar is that it should transmit the applied pulse efficiently into the ground. When the radar is designed to operate in the LFW the frequency band of operation is low so that the input pulse duration can become comparable to the propagation time of the pulse to the target and back again. With such a system any multiple reflections or "ringing" of the input signal on the antenna effectively extends the duration of the transmitted signal so that the wanted low level reflected signal is masked.

Effective coupling of the transmitted energy into the ground is achieved simply by lying the antenna on the surface of the ground, as shown by the following simple argument. Consider an antenna that is designed to respond to the horizontal electric field (e.g., a dipole), and is located an infinitesimal distance above the ground. Since the characteristic impedance of the ground is at most frequencies much lower than the characteristic impedance of free space, the voltage reflection coefficient of the air-ground interface is $\rho \simeq -1$ for a wave normally incident from the air medium. In this case, the electric field of the direct and reflected waves interfere destructively. Since the reciprocity theorem states that the reaction of an electric element is proportional to the electric field at the current element, the voltage generated at the antenna terminals is small. Next let the wave incident on the interface come from below the surface, i.e., from the lossy or conducting medium. The voltage reflection coefficient in this case is $\rho \simeq +1$ and thus the electric field interferes constructively at the interface. The tangential electric field is continuous across the interface so that the response of a linear antenna on the surface of the conducting interface is approximately $1+\rho$ times that of the same antenna immersed in a homogeneous conducting medium (ρ in this case is the voltage reflection coefficient of the air-ground interface for signals arriving from within the ground). It follows that such antennas lying on the surface of the ground respond to signals arriving from within the ground and, by the reciprocity theorem, they transmit most of their energy into the earth (in reality some energy may be supplied to surface waves, which propagate along the earth-air interface). This results in what we call an "interface gain" which can be up to two times, or 6 dB for each dipole of a transmit-receive pair.

There is an additional effect which occurs on transmit. It will be seen later that it is convenient to feed the antennas with a voltage pulse, with the source impedance of the pulse generator chosen to give a desirable match to the input of the antenna. Propagation calculations made between

antennas in a homogeneous medium and driven by voltage pulses will be presented later. For a given input voltage, the current on the transmitting antenna (which determines the fields) is determined by the antenna input impedance. When the antenna is placed at the air ground interface and in electrical contact with the ground, the input impedance is approximately twice what it would be if it were immersed in the homogeneous medium (because of the removal of one conducting half space and because the antenna impedance in the homogeneous medium is much less than its impedance in free space; Burrell and Munk, 1976). Therefore the antenna current and the fields are reduced by 6 dB. The "interface gain" of about 6 dB acts to make up this apparent loss, and the net effect is that the "interface gain" for a dipole on transmit is about 0 dB. Therefore, because of the voltage pulse input we use in our propagation calculations, the interface gain is about 0 dB for the transmitting dipole. The interface gain is 6 dB for the receiving dipole.

This can be cast into a somewhat clearer picture in terms of the reciprocity theorem given in this case by

$$\int_{L_1} \bar{I}_1 \cdot \bar{E}_2 \, d\ell = \int_{L_2} \bar{I}_2 \cdot \bar{E}_1 \, d\ell \qquad (14)$$

where $\bar{E}_1$ is the field at the second antenna caused by the current I_1 flowing on the first antenna, and

$\bar{E}_2$ is the field at the first antenna caused by the current I_2 flowing on the second antenna.

If the two antennas are widely separated, there is no change in $\bar{I}_2$ if the air-ground interface is inserted at the position of the first antenna. However the fields of $\bar{I}_2$ at the interface are now given by

$$E_2(1+\rho) \sim 2E_2 \, . \qquad (15)$$

The current in antenna 1 is halved when the source is a matched constant voltage source because the impedance has been doubled. The field $\bar{E}_1$ transmitted to the position of the second antenna is unchanged by use of Equation (14). Next examine the current and voltage induced on the first antenna by the second when this same interface is inserted at the position of the first antenna. By the same reasoning, I_2 is unchanged and E_2 is doubled. The open circuit voltage induced in the first antenna is simply $\int \bar{E}_2 \cdot d\bar{\ell}$, which is now twice the open circuit voltage in the homogeneous media. These effects have been verified on a limited scale by numerical results where the interface has been included via the Sommerfeld integral.

An important advantage of the effective coupling to the ground when the antenna is lying on the surface is that the antenna is insensitive to signal sources or reflections from objects above the ground. This is important because most noise sources are above the ground.

In an efficient system the antenna must be properly matched to the feedline. There are two ways in which a radiating element can be matched. These can be seen by considering the behavior of the radiating element on transmission (Bates, 1967):

1) The reflections from the driving point and the various physical discontinuities on the element are made to cancel in the transmission line which feeds the element.

2) The element is constructed so that there is a smooth transition from the feedline into the medium. Consequently only outward traveling waves exist on the antenna when it is transmitting.

Narrow band antennas are usually matched by the first method (a dipole is the simplest example of this). The first method can be made effective over a limited frequency range (e.g., a fat dipole). The second of the above two methods is the one which is most suitable for achieving efficient transmission of transients which have bandwidths of several decades of frequency (Bates, 1967; Burrell, 1971, Ch. 8; Bates and Burrell, 1972).

The first method of matching is equivalent to enforcing the well known conjugate impedance match

$$Z_{source} = Z^*_{antenna} \tag{16}$$

for all frequencies for which the input signal has significant energy. While this approach produces a match on the feed line, it causes multiple reflections on the antenna structure which produces a distorted radiated pulse. As we will see later, if the input pulse is carefully designed, these reflections on the antenna can be made to cancel each other. The majority of narrow band matching networks (e.g., stubs) utilize this principle.

The second method of matching requires that there be no reflections from the antenna, i.e.,

$$Z_{source} = Z_{antenna} \tag{17}$$

which, in general, conflicts with Equation (16) since efficiency is a design criterion. It follows that for efficient and faithful transmission of pulses, both the feedline and the antenna must have real

impedances for all frequencies for which the input pulse has sufficient energy. This is a common constraint for the transmission line design, but is an unusual and difficult constraint to meet for antennas required to transmit or receive signal bandwidths of several decades.

An additional constraint for faithful transmission is that the antenna must have a phase center of radiation which does not change position rapidly with frequency (the phase center is the apparent source of radiation). It is this requirement which precludes the use of spirals and log-periodic antennas for transient transmission (Collin and Zucker, 1969, sec. 22.5). This requirement also insists that the input to the antenna be carefully balanced. Any radiation from an unbalanced feed line will cause the phase center to shift.

The Dipole Antenna as a Transient Radiating Element

It turns out that the simplest of all radiating elements, the dipole, is particularly suitable for use in an underground radar system when it is in electrical contact with the ground. The dipole has a phase center which is constant with frequency. The characteristic impedance varies only slowly along the dipole, so that a current pulse propagates along the dipole almost undistorted.* The reflection due to the slowly changing characteristic impedance is so small that it can only be detected indirectly (Burrell, 1972). The dipole has an important practical advantage in that it is a simple antenna to store, and is relatively easy to position on the ground. Any other antenna of the required size would be too cumbersome to be practical.

A dipole has two discontinuities which are potential sources of reflections, the feedpoint and the open circuited ends. It is the reflections from these discontinuities which give the dipole its frequency sensitivity. For the dipole to be a good transient antenna these reflections must be eliminated. The discontinuity at the feedpoint can be minimized by feeding the dipole with a transmission line whose characteristic impedance matches the surge impedance of the dipole (Ross, 1967) (which for free space varies with the pulse duration; Burrell, 1971, sec. 5.4.2)**. Eliminating the reflection from the ends of the

*The dipole can be considered as a non-uniform transmission line whose inductances and capacitances per unit length, and hence the characteristic impedance, vary along the line (Schelkunoff and Friis, 1952). This characteristic impedance for a cylindrical dipole increases as the distance from the feed terminals increases.

**The surge impedance is the apparent impedance terminating the transmission line as seen by the pulse. Its value depends only upon the "average characteristic impedance" of the dipole for a distance $v\tau/2$ from the feedpoint, where τ is the input pulse duration and v is the velocity of propagation of the pulse on the dipole.

dipole is not as simple when the dipole is in free space. One approach is to fold the dipole to form a loop, and load the ends with the appropriate value of resistor (Dion, 1970; Young, 1975).

The preceding discussion refers to techniques used for dipoles in free space, and for input pulses which are short compared to the propagation time along the dipole. These techniques are also applicable to radars which are designed to operate in the HFW, as will be discussed later. For radars which must operate in the LFW the frequency band of operation is necessarily low and the duration of the input pulse is many times its propagation time along the antenna. Fortuitously, when the dipole is used for transmission underground, the conducting earth medium can be used to advantage in antenna matching. When a dipole is placed in electrical contact with a conducting medium, conduction currents made a significant contribution to the dipole input impedance. The effect of the conduction currents is to reduce the frequency sensitivity of the dipole impedance. The input resistance tends to a finite value at zero frequency, which is the d.c. resistance measured between the terminals (conduction currents are the only currents present at zero frequency). The reactance is small and becomes zero at zero frequency. As a result an almost reflection free match from zero frequency to the upper spectral limit of an LFW radar pulse can be obtained for the dipole simply by arranging continuous electrical contact with the ground.

Physically what happens is that the shunt resistance of the conducting medium attenuates the currents propagating along the dipole thereby reducing the reflections which occur from the ends. When the dipole is short, the attenuation is not sufficient to reduce the reflections from the ends to an insignificant amplitude. The reflection from the end of the dipole corresponds to a resistive load at that point since there is no significant energy storage mechanism. If, in addition, the total path from the feed to the end of the dipole and back is very small in terms of wavelengths, this reflected component is either in phase or out of phase with the signal feeding the dipole depending on the sign of the reflected wave at the end of the dipole. Thus the impedance is nearly a real quantity. This reflected wave experiences a more significant phase shift as either the dipole becomes longer or the frequency is increased, and then the reactive component of impedance becomes significant. Note that this discussion refers to a short dipole in a conducting medium, in which case the current is in phase with the voltage as $\omega \to 0$ (Equation (8)) giving a real impedance, whereas in the more familiar free space case the current is 90° out of phase with the voltage as $\omega \to 0$. The presence of these multiple reflections on short antennas does not contravene the design criterion discussed earlier which required outward traveling waves only to exist on the antenna. Since the waves traveling inward after reflection from the ends of the dipole are lower in amplitude than the original outward traveling waves, and since they overlap in time very closely, the outward traveling waves dominate and effectively there are only outward traveling waves present on the dipole. When the antenna becomes long and the medium conductivity high, the attenuation of the pulse propagating along the dipole is so high that the end reflections will be insignificant and the design criterion is satisfied almost exactly.

Plots of the input impedance of bare 0.002 m radius copper wire dipoles immersed in infinite homogeneous media are presented in Figures 7-9. The impedances are computed by the moment method (Richmond, 1974a, 1974b). Notice the almost constant values for the input resistance when the frequency is below a certain value which depends upon the antenna length 2ℓ and the medium conductivity σ. It will be seen later that the frequency band of operation of an LFW radar will usually be within the region of constant input resistance. The reactance is observed to be much lower than the input resistance at low frequencies, which is where most of the pulse energy will be concentrated. It is interesting to note that for the range of frequencies for which data is presented, the antenna reactance never exceeds the antenna resistance, regardless of the antenna length. However, at high frequencies the reactance becomes comparable to the resistance, and the consequent deterioration in the impedance match to the pulse generator means that there is an upper limit on the length of antenna which may be used for a specific application. For example, the cut-off frequency of the LFW for a depth of penetration of 100 m in a medium having a conductivity of 0.1 mhos/m is f_m = 940 Hz. For a 50 m long antenna, the antenna reactance is about 7% of the antenna resistance at this frequency. This is probably not sufficient to cause a serious matching problem. It will be shown later that for an LFW radar the delay of the received signal is usually insufficient for it to be completely separated in time from the transmitted signal when the transmitted signal is a pulse bandlimited at f_m. For this reason it is proposed that the input signal have frequency components up to about 10 f_m, which means that the input signal is 10 times shorter. This allows separation of the transmitted and received signals. The penalty is an increase in attenuation, and this will be discussed later. If this procedure is used, then for the example quoted above, a pulse with significant energy up to about 9.4 KHz would be applied to the antenna. At this frequency the antenna reactance becomes comparable to the antenna resistance and a matching problem could be encountered at the upper end of the frequency band, although this will be somewhat alleviated by the increase in antenna resistance when the antenna is located at the air-ground interface (shown later). Several calculations made with media of other conductivities with a radar range d=100 m give similar results to the above example suggesting that 50 m is the longest antenna which should be used for an LFW radar operating in this range.

Finally it is noted that a practical generator impedance equal to a pure resistance can be achieved in the pulser design simply by setting the characteristic impedance of its associated delay line equal to the antenna resistance.

Placing the antenna on the surface of the earth will alter its input impedance. Since the upper half space is a high impedance medium, it is reasonable to expect the input resistance to be twice the values given by Figures 7-9. We did a sample computation using the Array Scanning Method (Burrell and Munk, 1976) at 100 Hz for a 1000 m long dipole buried in a half space of constitutive parameters σ=.01 mhos/m and ε_r=4, and the results indicated that this assumption is valid. The computation also

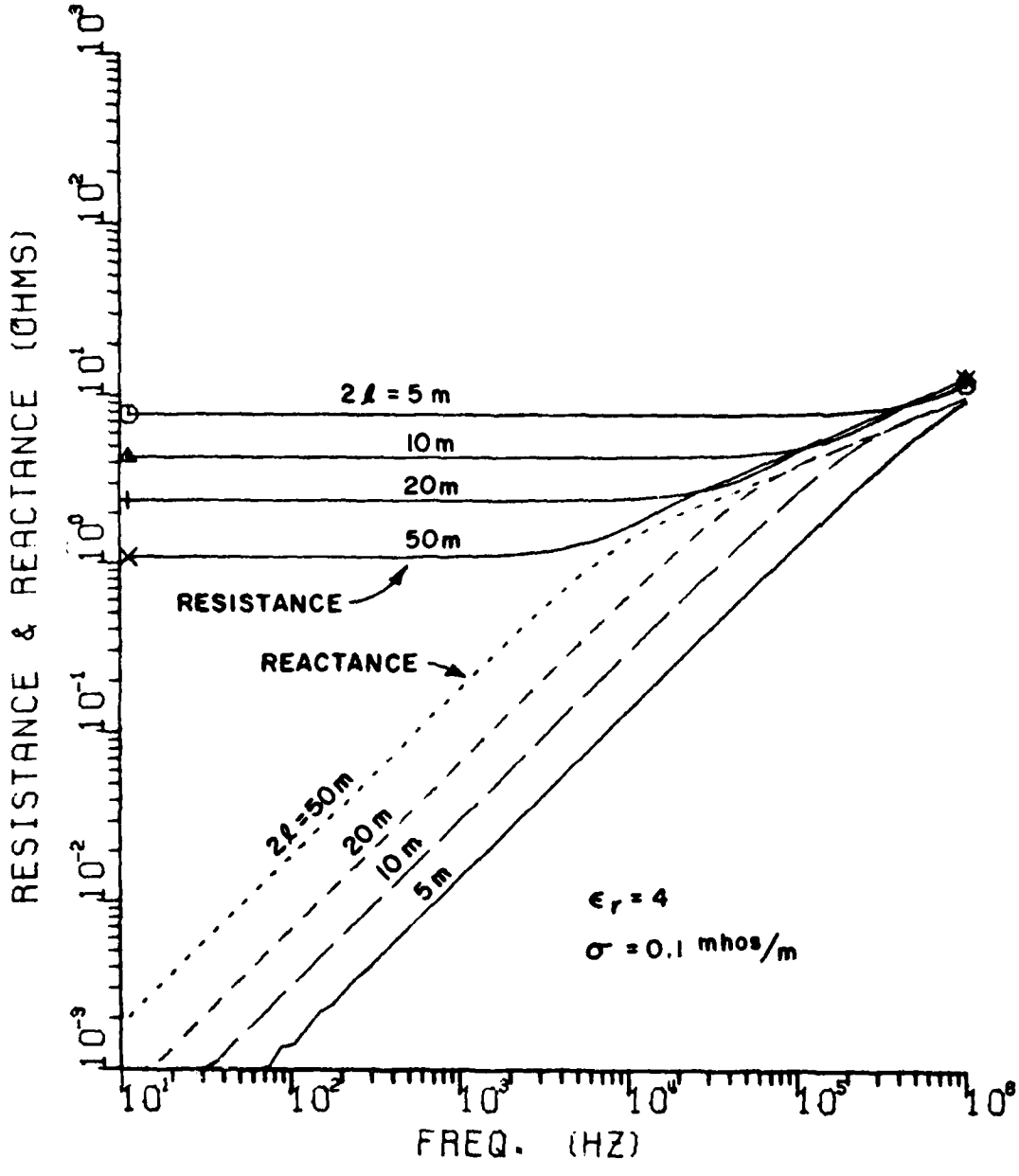

Figure 7. Input impedance of 0.002 m radius bare copper wire dipole antennas in an infinite homogeneous medium.

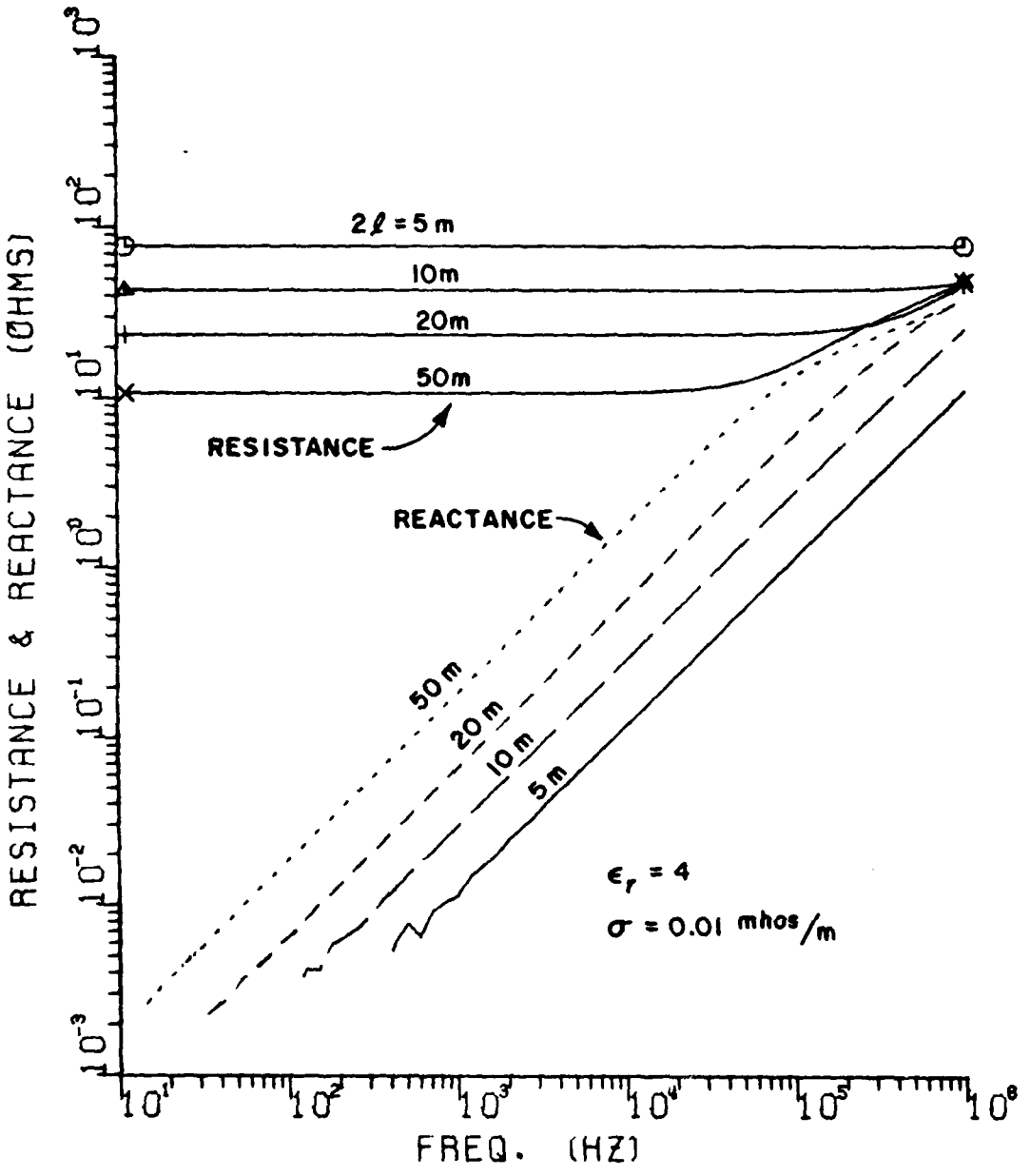

Figure 8. Input impedance of 0.002 m radius bare copper wire dipole antennas in an infinite homogeneous medium.

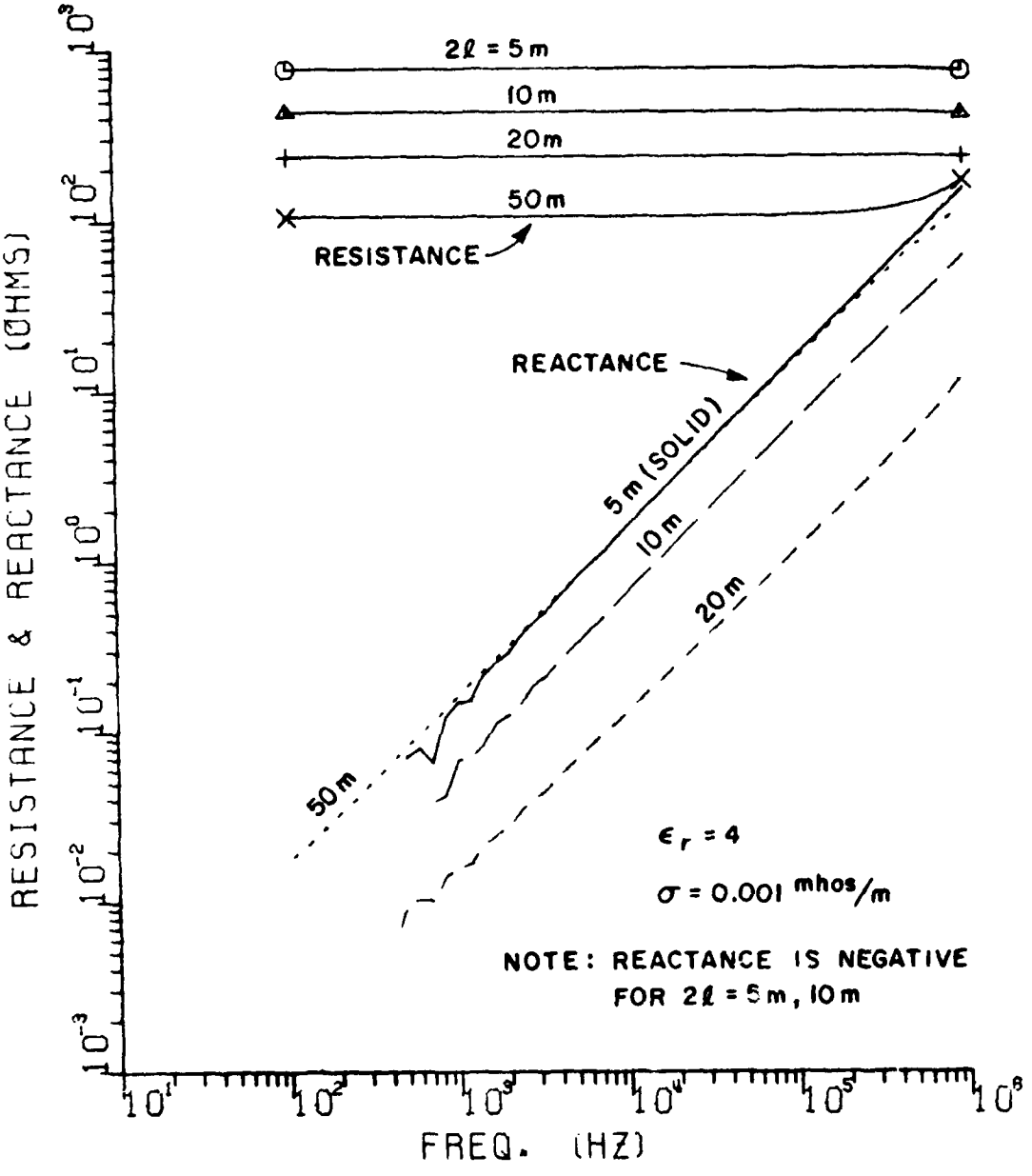

Figure 9. Input impedance of 0.002 m radius bare copper wire dipole antennas in an infinite homogeneous medium.

indicated that the reactance was the same as for an infinite medium. This relatively lower reactance means that in practice we can expect the dipole to be even better matched than Figures 7-9 indicate. The input impedances presented in Figures 7-9 are valid only for 0.002 m radius antennas. Altering the radius alters the surface area in contact with the ground thereby changing the input impedance. A curve illustrating the change in input impedance as the radius changes is shown in Figure 10, and it is seen that the input impedance is not a sensitive function of antenna radius. We established that the source resistance of the pulse generator should be set equal to the input resistance of the antenna. In practice this could be determined simply for the constructed antenna with a d.c. ohm-meter. Usually it will not be practical to bury the antenna completely in the ground to ensure that continuous conducting contact is made along the whole length of the antenna. We will be investigating methods of achieving satisfactory electrical contact with the antenna lying on the surface. One of these methods involves driving conducting pins into the ground at regular intervals along the length of the antenna. Another method consists of covering the antenna with a mud solution.

The discussion in this section has mainly been concerned with antennas for an LFW radar. HFW radar antennas are less critical with respect to ground contact but pose their own particular problems with respect to antenna matching. This will be seen in subsequent sections. We will be seeking optimum designs for such radar antennas in our future research.

Again, we repeat that all of the preceding results are for the case of a constant voltage source placed at the terminals of the antenna. For a pulser constructed using a delay line, this represents a practical assumption. For other applications, perhaps some cw tecnnique, these results can be transformed to any sort of a driving function desired by the use of the antenna impedance results given in the preceding section.

5. THE ELECTRIC FIELD INTENSITY OF FINITE LENGTH WIRE DIPOLES IN A HOMOGENEOUS MEDIUM

The fields of a practical electric dipole differ from those of the elementary dipole presented in Section 2. Figure 11 shows the magnitude of the parallel electric field measured at a point 30 m from a 0.1 m long, 0.0001 m radius perfectly conducting dipole buried in homogeneous media. The solution was by a sinusoidal Galerkin moment method (Richmond, 1974a). The dipole is excited at its center by a 1 volt generator. This would be equivalent to a 2 volt generator voltage with an internal impedance equal to the antenna impedance. As we have observed, in the LFW, this is a practical impedance match when the antenna is in electrical contact with the conducting ground. Note that the curves for the electric field in the various media display the same characteristics as those for the current element shown in Figures 2-5. The frequency responses are identical in shape up to the LFW cutoff frequency, and the depth of the minima agree to within a few dB. In the HFW $|E_\theta|$ is seen to increase at a faster rate as the frequency increases than do the corresponding curves for the current

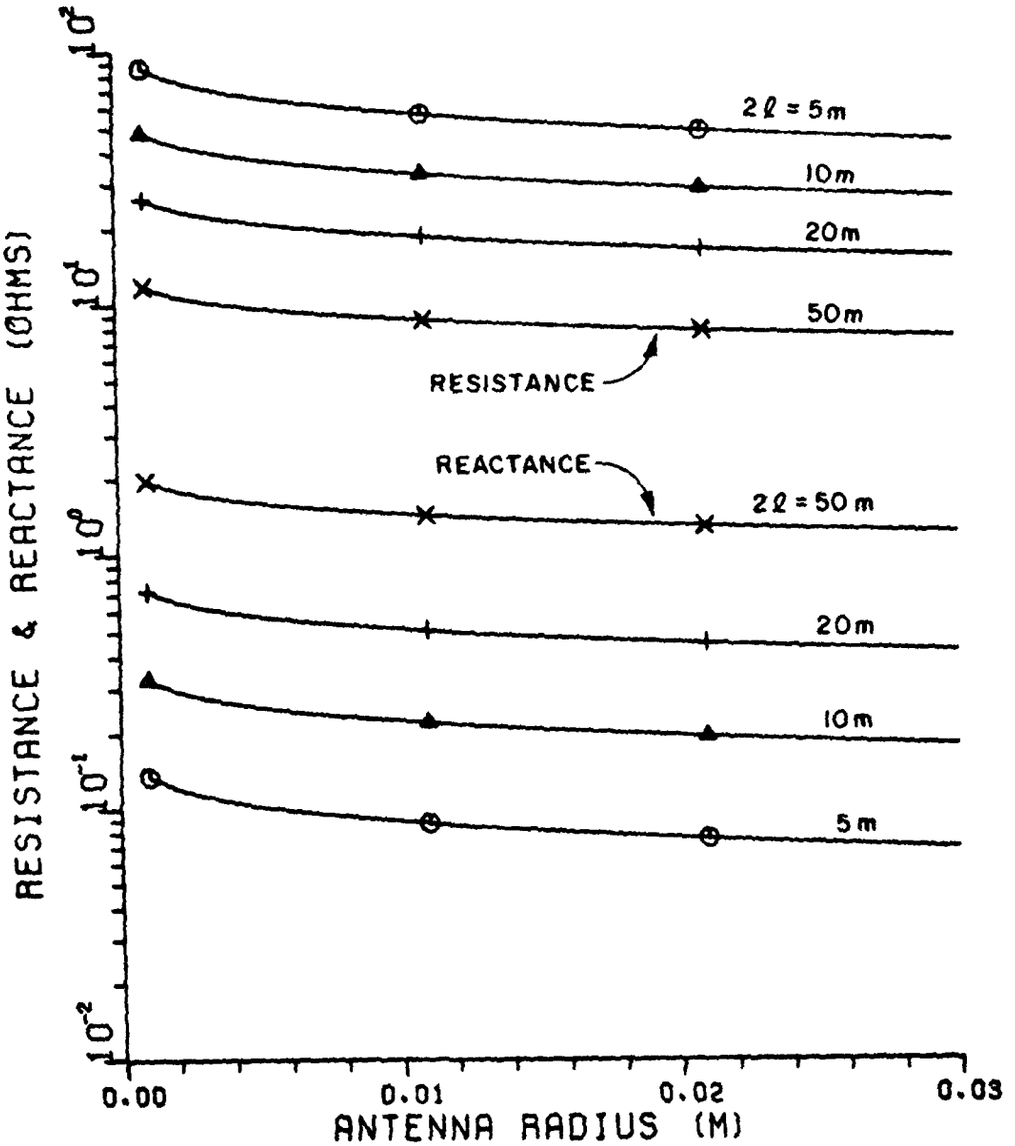

Figure 10. Illustrating the change in input impedance of bare copper wire dipole antennas as the radius changes. σ=0.01 mhos/m and ϵ_r=4.

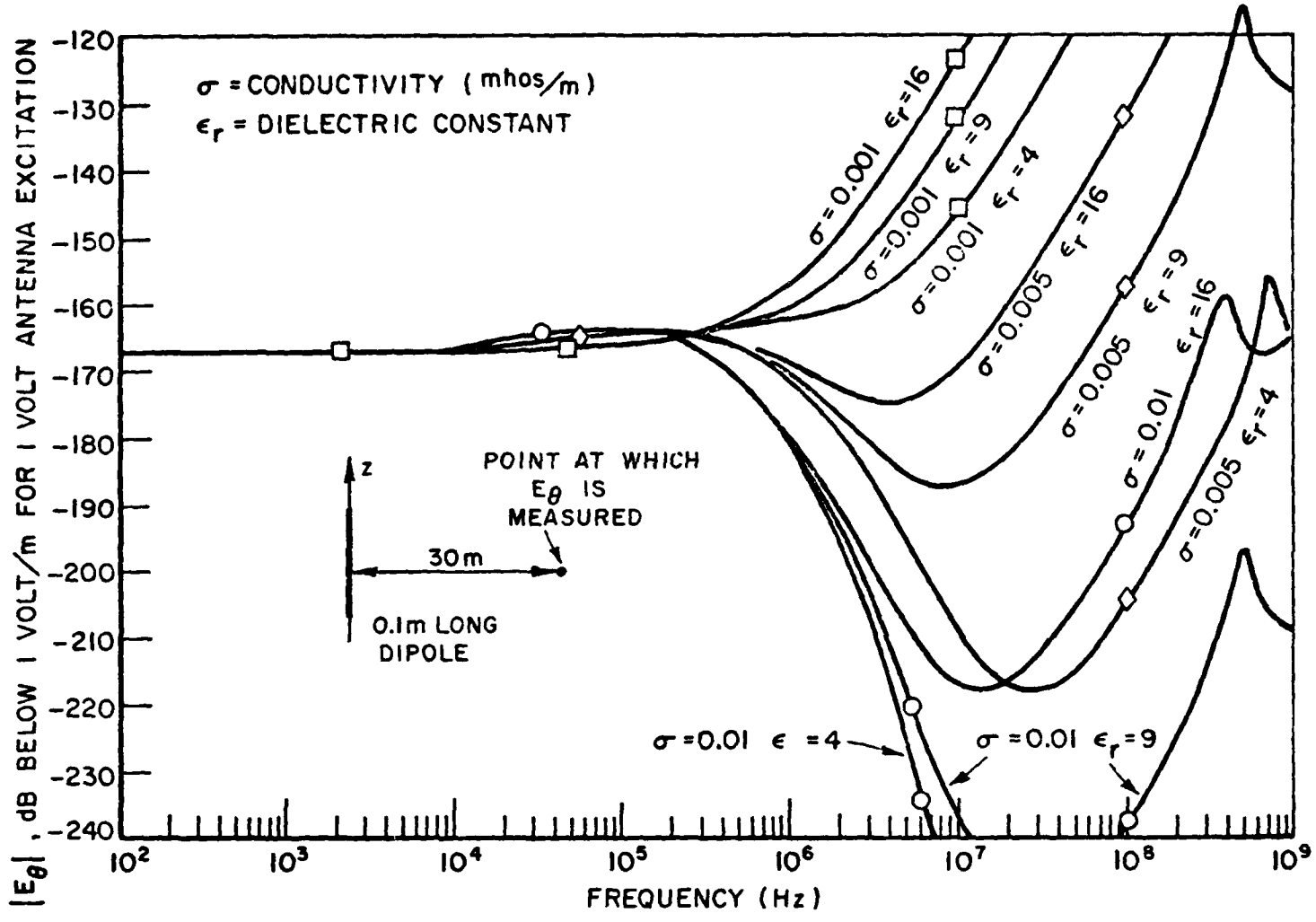

Figure 11. Magnitude of electric field strength of 0.1 m long, 0.0001 m radius perfectly conducting dipole in homogeneous media. The distance to the measurement point is 30 m.

element shown in Figures 2-5. The dipole used is small and since in the HFW all media behave as lossy dielectrics, the dipole impedance does not behave in the way shown in Figures 7-9, but follows the familiar free space behavior. As a result the magnitude of the input impedance of the dipole becomes smaller as the frequency increases so that the current at the dipole terminals increases as the frequency increases. Hence in the HFW $|E_\theta|$ increases at a faster rate than it does for the elementary dipole which assumes a constant input terminal current. At low frequencies $|E_\theta|$ for the 0.1 m dipole is seen to be independent of frequency: this is the same as for the current element because the input impedance is constant at low frequencies, as was shown in Section 4. The practical dipole also exhibits resonance, and this is seen as a peak in the frequency response for several of the dipoles whose frequency responses are shown in Figure 11.

The importance of electrical contact of the antenna with the ground when the radar operates in the LFW is clearly shown in Figure 12, where the magnitude of the electric field of insulated and uninsulated dipoles is compared. A severe signal loss occurs if conducting electrical contact is not made with the ground in the LFW. Note that at low frequencies when the dipole is insulated, the electric field magnitude decays at a rate of 20 dB/decade of frequency decrease. The physical explanation is that the insulation acts as a capacitor in series with the conducting earth, and the conduction currents are limited by the capacitor reactance which decreases as 1/f. It is noted that it would be possible to achieve results using an insulated antenna which are comparable to those for the antenna in electrical contact with the ground by using a reactive element in the generator impedance at any single frequency. However if a broadband match is required this would at best represent a very difficult task, especially when high voltage pulse generators are required. In the HFW, the concept of electrical contact with the ground loses its advantage in that the magnitude of the reactance is comparable to that of the resistance. This represents one of the problems for operation in the HFW and it becomes necessary to load the antenna structure in the form of resistive loads (or absorbers).

Thus in the HFW, the dipoles may be either uninsulated or insulated; if insulated there is the advantage of the increased mobility of the antenna system. Note in Figure 12 the small signal loss ($\lesssim$ 4 dB) caused by the insulation. This is attributed to the insulated antenna having a higher input impedance and hence a lower impressed current from the 1 volt generator assumed in the calculations.

Figure 13 compares the electric field strengths of dipoles of different lengths for a homogeneous medium σ=.001 mhos/m and ε_r=4. Note that for these medium parameters the fields of a current element (Figure 2) and a short dipole (Figure 11) do not exhibit a null in the frequency response. In Figure 13 the electric field decreases in magnitude as the dipole length decreases because of the decreased dipole moment and the increasing input impedance. This means that when the radar operates in the HFW and the antennas are operated in the resonance region (which is recommended later in Section 8), the signal increase suggested by Figure 11 is not obtained. However the general behavior of each curve in Figure 13 is very similar to the relevant curve in Figure 11.

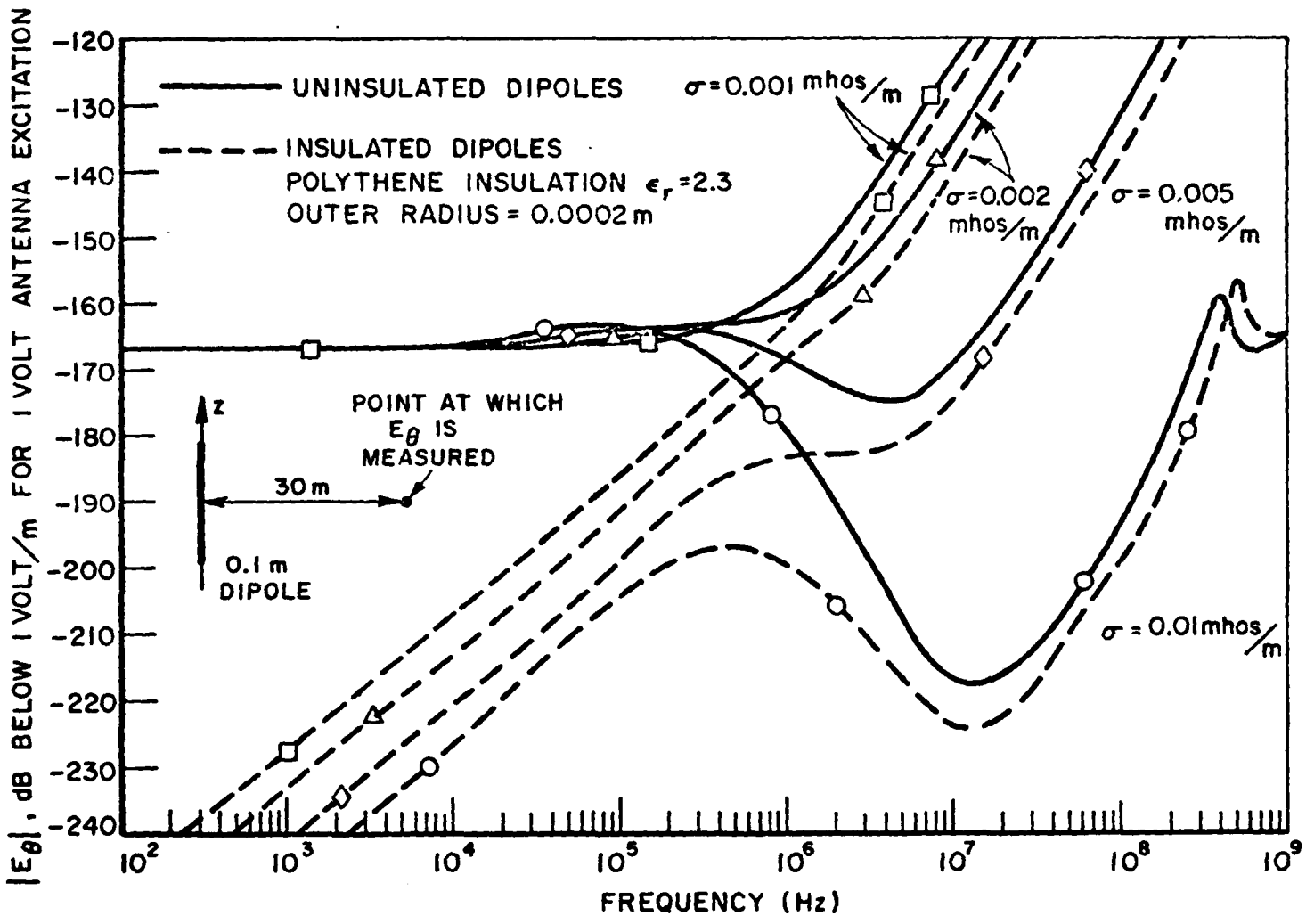

Figure 12. Magnitude of electric field strength 30 m from 0.1 m long, 0.0001 m radius dipoles in homogeneous media. Results are presented for insulated and uninsulated dipoles.

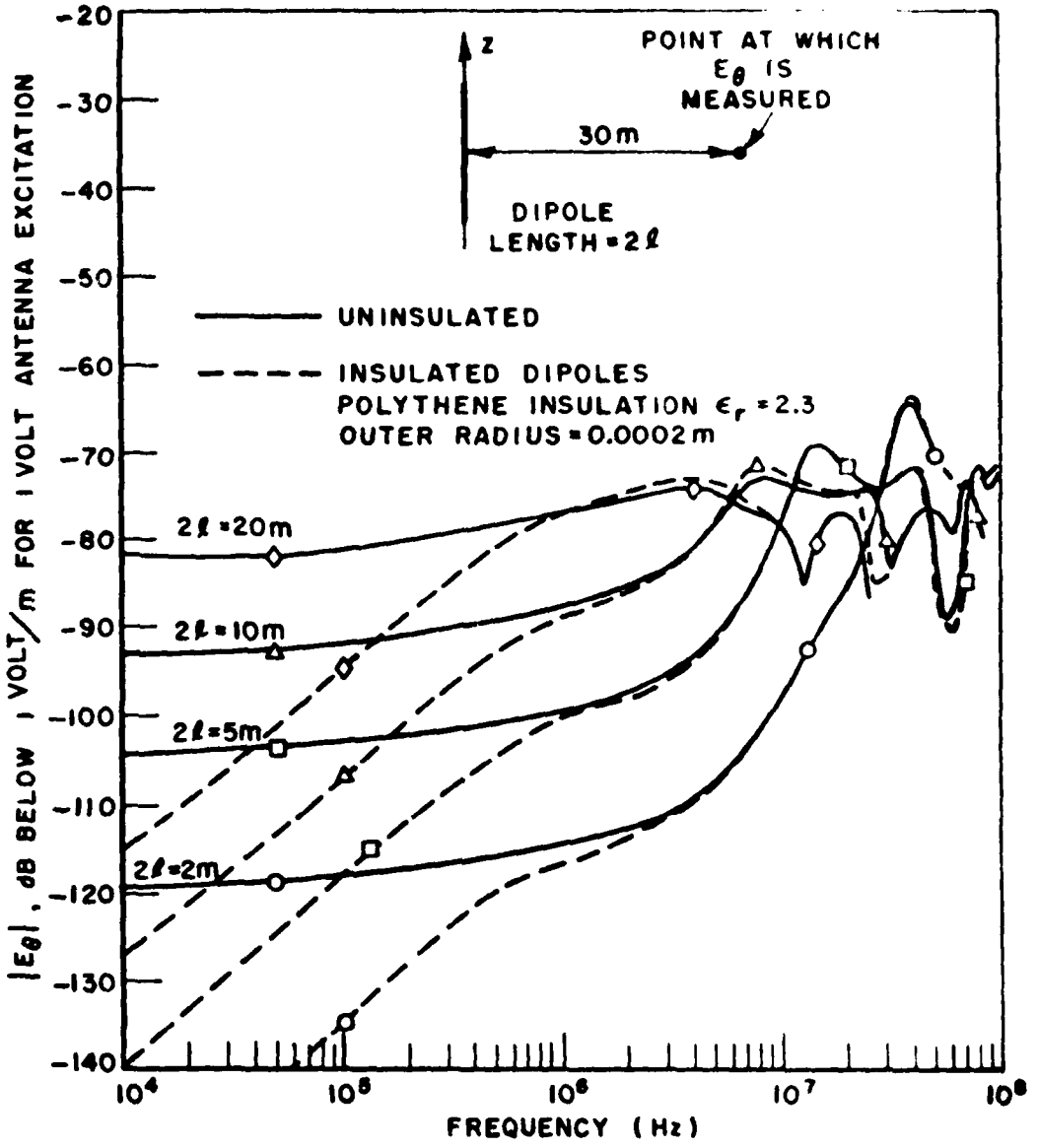

Figure 13. Magnitude of electric field strength 30m from 0.0001m radius perfectly conducting dipoles in a homogeneous medium of ϵ_r=4, σ=0.001 mhos/m. Results are presented for dipole lengths of 2m, 5m, 10m, and 20m.

Note that the dipole resonance, which is relatively sharp for the 2m long dipole, becomes less prominent and broadens as the dipole lengthens and the resonant frequency moves towards the LFW.

Figure 14 shows the variation of electric field strength with dipole length when the medium is more lossy, σ=0.005 mhos/m and ϵ_r=9. For these parameters the resonance of the 20m antenna is completely damped out. Again note that the general behavior of the frequency response is similar to that shown for the short dipole and the same constitutive parameters in Figure 11.

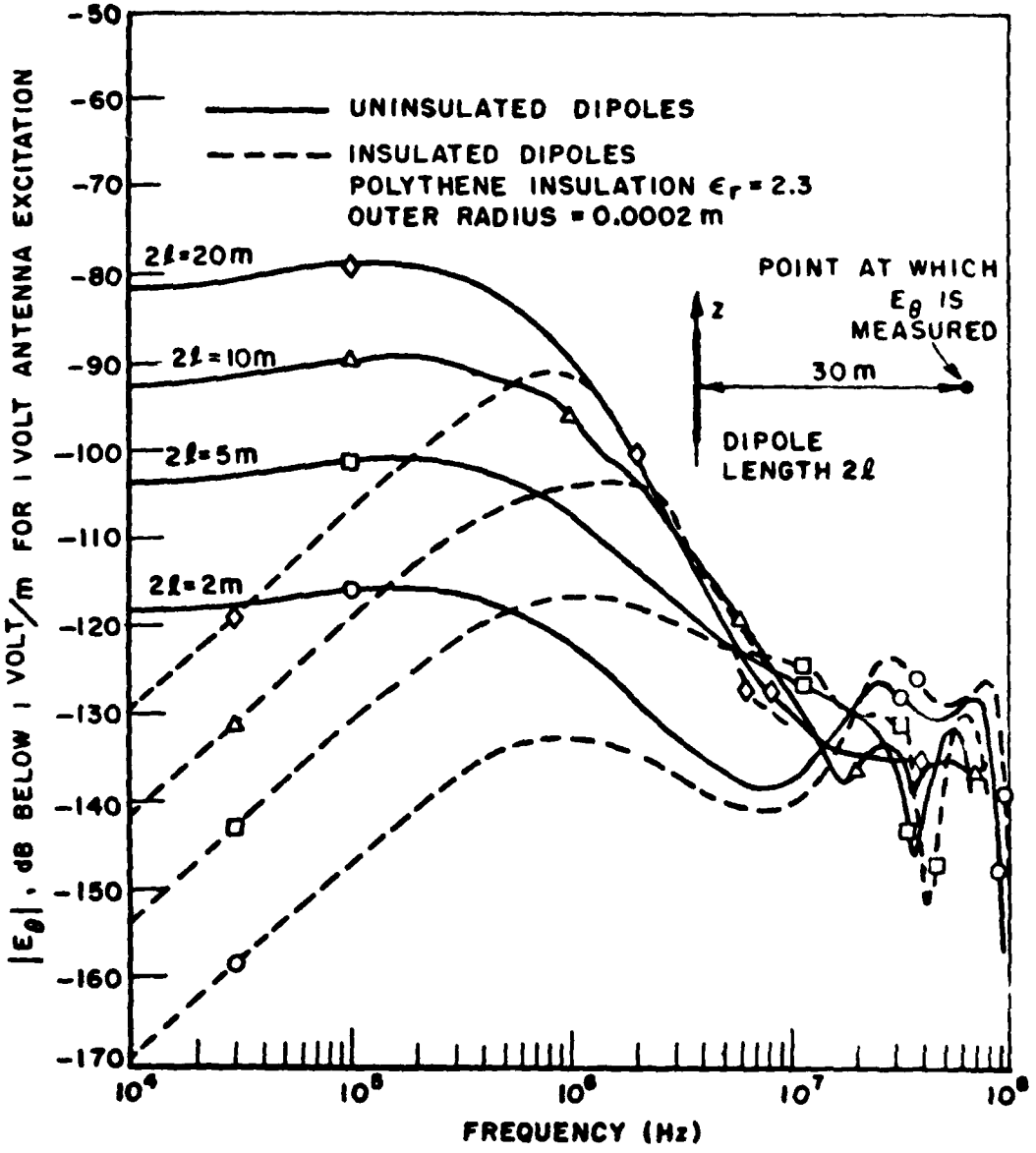

Figure 14. Magnitude of electric field strength 30m from 0.0001m radius perfectly conducting dipoles in a homogeneous medium of ϵ_r=4, σ=.005 mhos/m. Results are presented for dipole lengths of 2m, 5m, 10m and 20m.

The loss in signal at low frequencies when the dipole is insulated is again shown clearly in Figures 13 and 14. Notice that in Figures 13 and 14 that when the dipole is electrically shorter than a quarter wavelength, and the frequencies are within the LFW, the electric field strength increases 11 dB for each octave increase in the antenna length.

6. A COMPUTER MODEL FOR THE ANTENNA-MEDIUM PROPAGATION MECHANISMS

The radar system we are considering consists either of a dipole antenna at the surface of the ground (if the same antenna is used for both transmitting and receiving) or of two crossed dipoles at the surface of the ground (if separate antennas are used for transmitting and receiving and isolation between the two antennas is required). The target of interest, a tunnel, is buried below the antenna. Figure 15 depicts such a system

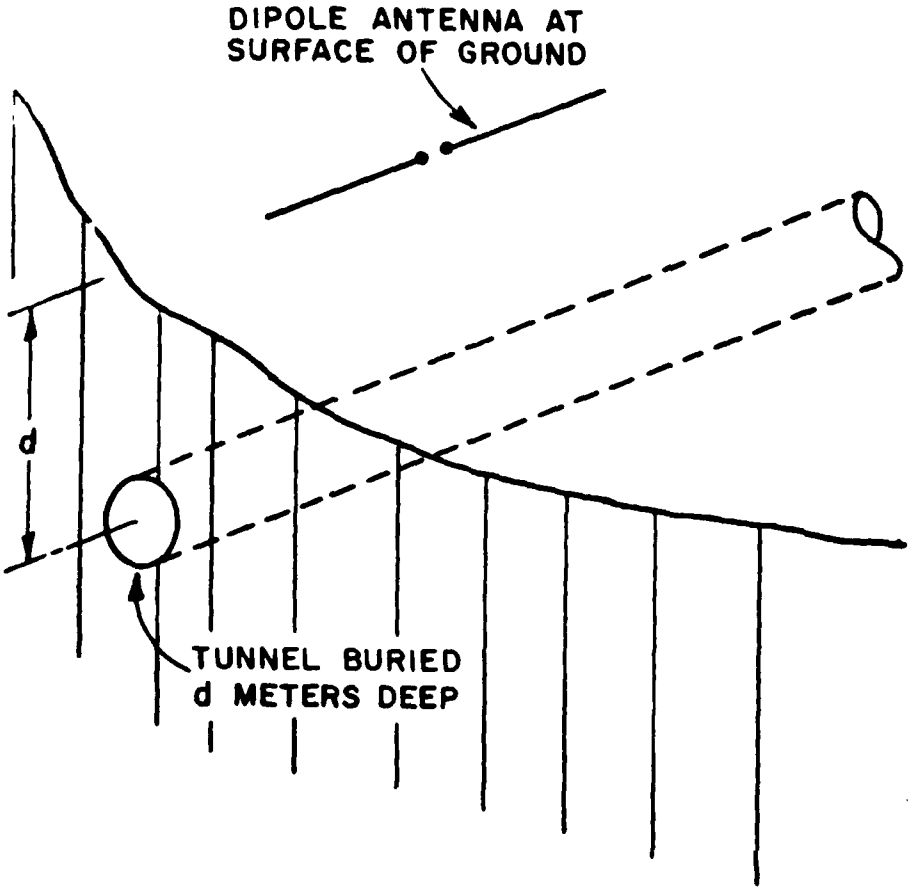

Figure 15. Radar antenna at surface of ground and tunnel target.

when a single dipole antenna is used. We require a model from which we can obtain the propagation mechanisms of pulse signals from dipole antennas in the ground medium separately from the scattering mechanisms of the target. This separation of target scattering and propagation mechanisms is necessary to simplify the study by reducing the number of variable parameters to manageable proportions. It also leads to a better understanding of the various propagation and scattering mechanisms which combine to produce the total system response. We have done this in the following way.

Figure 16a shows the radar when the target (the tunnel) is replaced by a perfectly reflecting plane infinite interface parallel with the surface of the ground. By applying image theory the model of Figure 16(b) can be constructed. Next we have simplified the model to that shown in Figure 16(c)

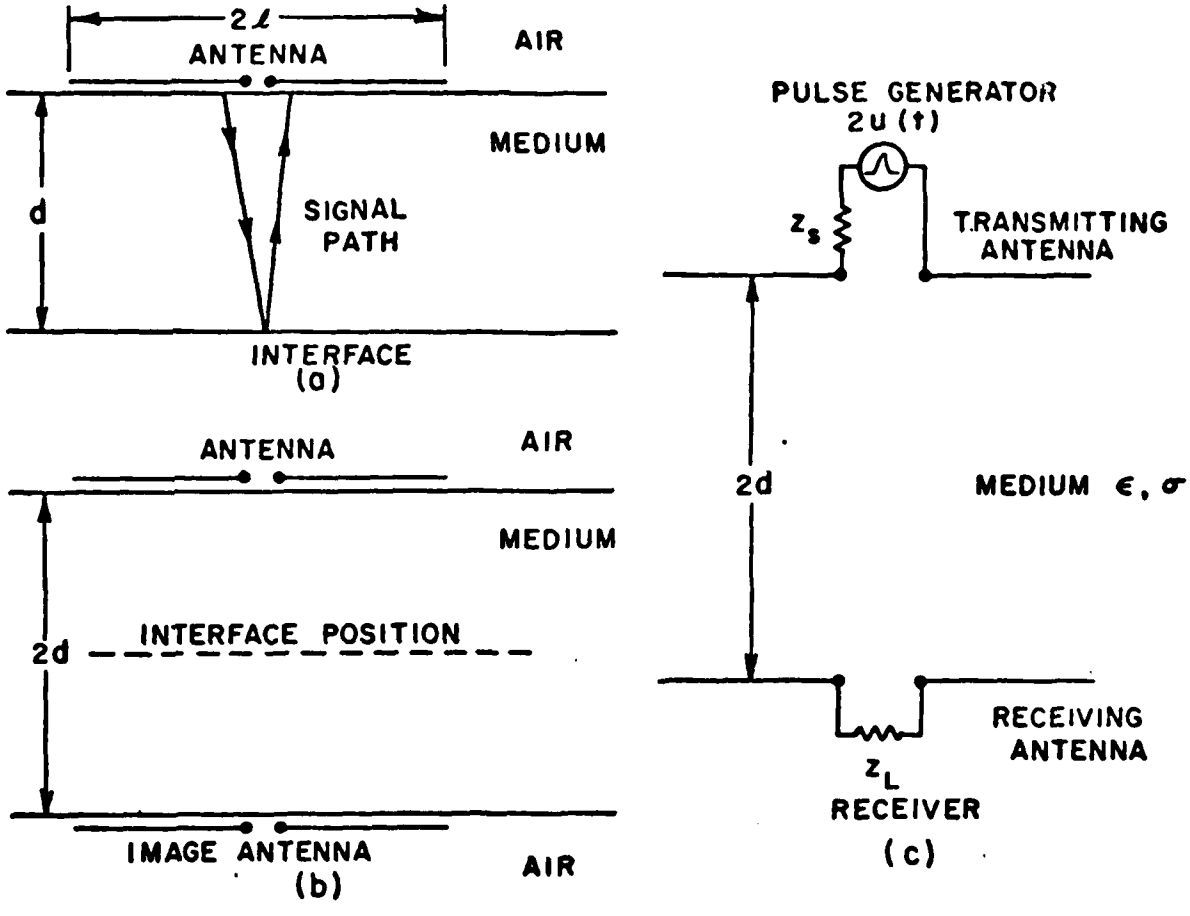

Figure 16. Development of a model for analysis of pulse propagation into the earth. (a) Reflection from an antenna d meters deep. (b) Model of reflection from a perfectly reflecting interface. (c) Simplified model of reflection from a perfectly reflecting interface.

by replacing the air with homogeneous medium. This is justified because simple reasoning presented earlier in Section 4 showed that the major effect of the interface is to introduce an "interface gain" whose magnitude depends upon the Fresnel reflection coefficient at the interface. By adopting the model of Figure 16(c) we avoid the time consuming computation of Sommerfeld integrals required to account for the air-ground interface. The effect of scattering from a target such as a tunnel can then be included by normalizing the result from the scattering solution of the tunnel by the scattering from an infinite ground plane. This will be described in a forthcoming report.

As shown in Figure 16(c) we have modelled the pulse generator by its Thevenin equivalent circuit. The Thevenin generator voltage is twice the output voltage, because in antenna engineering it is common to refer to the output voltage of a generator as the voltage delivered to a load whose impedance equals the generator source impedance Z_s. In general the voltage appearing across the antenna terminals will not be u(t) because the antenna impedance will vary with frequency. However if the LFW is used, the antenna impedance is practically independent of frequency and for this case the voltage applied to the antenna terminals will be approximately u(t).

To obtain both the transmission and reflection characteristics of the pair of parallel non-displaced dipole antennas in Figure 16(c) to the input signal u(t), the z-matrix of the two port network comprising the dipoles and the medium was computed for 512 equally spaced frequencies up to a maximum frequency which was about 2.5 times the highest frequency for which the input pulse had significant energy. The resulting integral equation was solved by the moment method using a piecewise sinusoidal expansion for the current distribution (Richmond, 1974a, 1974b). From the z matrix data computed as a function of frequency ($Z_{11}(f)$ and $Z_{12}(f)$), the signal reflected from the transmitting dipole can be obtained from the reflection coefficient $\rho(f)$. $\rho(f)$ is obtained from the input impedance $Z_{in}(f)$:

$$\rho(f) = \frac{Z_{in}(f) - Z_s}{Z_{in}(f) + Z_s} \tag{18}$$

where

$$Z_{in}(f) = Z_{11}(f) - \frac{Z_{12}(f)^2}{Z_L + Z_{11}(f)} \tag{19}$$

The spectrum of the reflected signal $v_1(t)$ is $V_1(f)$ (where upper case roman letters are used for spectra and lower case letters for time domain signals) and is obtained from

$$V_1(f) = \rho(f)\, U(f) \tag{20}$$

where U(f) is the spectrum of the input signal u(t). Hence

$$v_1(t) = F^{-1}(V_1(f)) \tag{21}$$

where F^{-1} denotes the inverse Fourier transform. To obtain the signal received on the receiving dipole we have defined a transmission coefficient H(f) as follows

$$H(f) = \frac{V_2(f)}{U(f)} \tag{22}$$

where $V_2(f)$ is the spectrum of the received signal $v_2(t)$ which appears across the load impedance Z_L.

The transmission coefficient is given by

$$H(f) = \frac{2Z_{12}(f)Z_L}{(Z_{in}(f)+Z_s)(Z_{11}(f)+Z_s)} \tag{23}$$

and the received signal $v_2(t)$ by

$$v_2(t) = F^{-1}\{H(f)U(f)\} \,. \tag{24}$$

By storing the results of the computation (two elements of the z-matrix), the response of the system of the two antennas in the homogeneous medium can be readily evaluated for different input signals and different source and load impedances. Note that if only one dipole antenna is used, the signal at the terminals is $[v_1(t) + v_2(t)]$.

The received signal was computed using the FFT algorithm with 1024 sample points. Truncation error (Bergland, 1969) is all but eliminated when the frequency response is computed for all 512 frequencies as we have done. Both aliasing error (Bergland, 1969) and truncation error are reduced by using a signal whose spectrum magnitude decreases rapidly and smoothly with increasing frequency. For this reason we have often chosen a gaussian pulse as the input signal. Also, the outputs of many pulse generators are approximately gaussian in shape. Figure 17 shows a normalized gaussian pulse and its spectrum. The equation of this gaussian pulse is

$$u(t) = -5.5\, t^2/t_p^2 \tag{25}$$

where t_p is defined as the pulse duration.

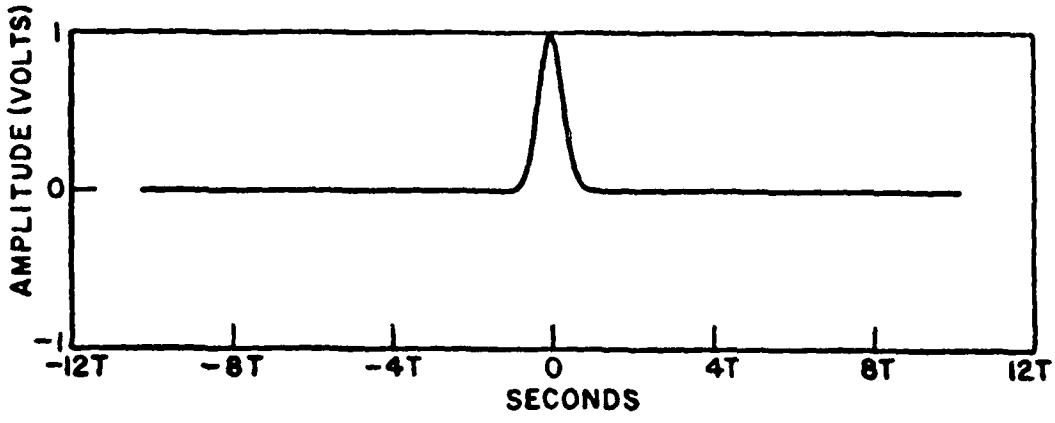

(a) INPUT PULSE, $t_p = T$ SECONDS

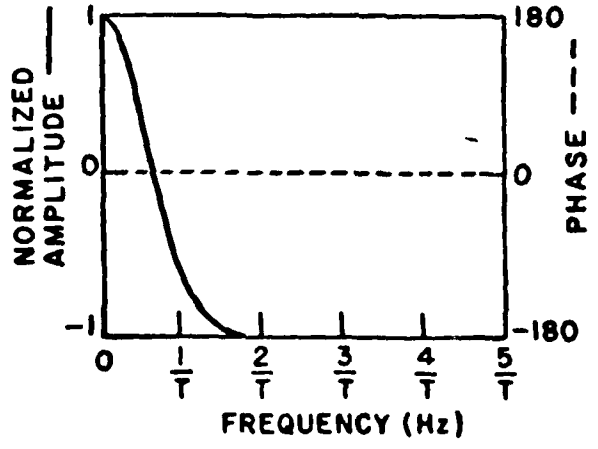

(b) INPUT PULSE SPECTRUM NORMALIZED TO 7.344 T VOLTS / Hz

Figure 17. (a) Normalized gaussian pulse and (b) its spectrum.

7. PULSE PROPAGATION IN THE LFW

Pulse propagation calculations have been made using the model of Figure 16(c) for antenna lengths ranging from 5m to 50m. These calculations were made using an input signal of fixed duration, and a set of universal attenuation curves has been constructed which describe the pulse attenuation in the medium. The important features of these curves are discussed. Next, consideration is given to the characteristics of the signal required for a practical radar, and the application of the universal curves to a practical radar design is discussed.

(1) Pulse Propagation for 100 μs Gaussian Pulses

For the radar ranges under consideration in this report, it was determined that the required design data could be obtained from a set of calculations in which the frequency response was calculated to 50 KHz, and the reflected and received signals were calculated for a gaussian pulse for which t_p = 100 μs (Burrell and Peters, 1976).

For each antenna and medium conductivity, values for the source impedance Z_S and the load impedance Z_L were chosen to minimize reflections of the input pulse from the antennas. The choice made was $Z_S = Z_L$ = d.c. input resistance of the antenna. Because the input resistance is almost constant at low frequencies, the value of the input resistance at the lowest computed frequency was used as the d.c. input resistance (which could not be computed with our computer program).

Figure 18 shows the normalized transmission transfer functions for transmission between matched 10m long dipoles spaced 240m apart in infinite homogeneous media. The relative dielectric constant ε_r used was 4 (the exact value of ε_r has negligible effect since the medium is a conductor), and the results for four different conductivities are shown. The -3 dB cutoff frequency (with respect to the amplitude at zero frequency) is slightly lower than that calculated from Equation (11) (e.g., 5900 Hz compared to 6527 Hz for $\sigma=10^{-2}$ mhos/m as depicted in Figure 18); however in our model the additional frequency dependence of the receiving antenna has slightly lowered the cutoff frequency. Because of the vagaries of the propagation path in practice this difference can be ignored.

Since the frequency response is effectively flat over the range of frequencies for which a 100 μs input pulse has significant energy (Figure 17) and the phase (although not shown in Figure 18 for clarity) is approximately linear,* Figure 18 shows that little distortion of the

*The phase characteristic for propagation through conducting media is proportional to $\sqrt{f}$, but at low frequencies, the small electrical spacing of the transmitting and receiving antennas make this effect unimportant.

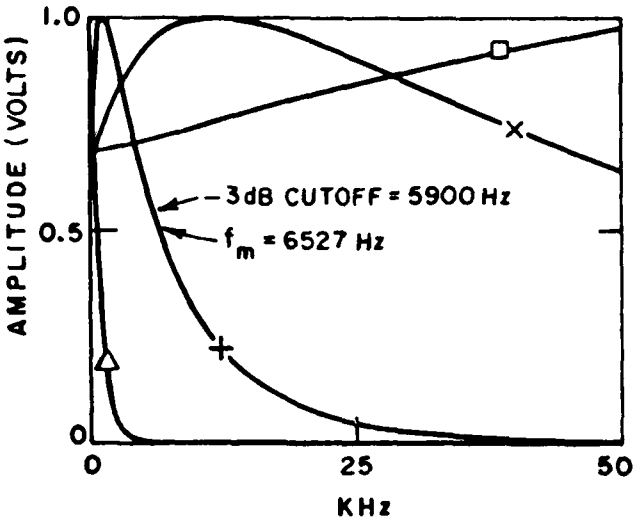

△ $\sigma = 0.1$ $z_s = 4.3\Omega$

\+ $\sigma = 0.01$ $z_s = 43.4\,\Omega$

× $\sigma = 0.001$ $z_s = 433.8\,\Omega$

□ $\sigma = 0.0001$ $z_s = 4337.3\,\Omega$

Figure 18. *Normalized frequency responses for transmission between two parallel 10m long dipoles 240m apart in homogeneous media of various conductivities. The difference between the -3 dB cutoff frequency (with respect to the amplitude at zero frequency) of the system of two dipoles is compared to* f_m *for* $\sigma = 10^{-2}$ mhos/m.

input pulse will occur except when σ is of the order of 0.1 mhos/m or greater. This is confirmed in Figure 19, which shows both the signals on the transmission line reflected from the transmitting antenna back towards the pulse generator, and the signal received on the receiving antenna. (The amplitudes in dB on these and subsequent plots are referred to the input pulse amplitude.) Therefore it is meaningful to define an attenuation factor A which is given by

$$A = V_r/V_i \tag{26}$$

where V_r = peak amplitude of received pulse

V_i = peak amplitude of input pulse.

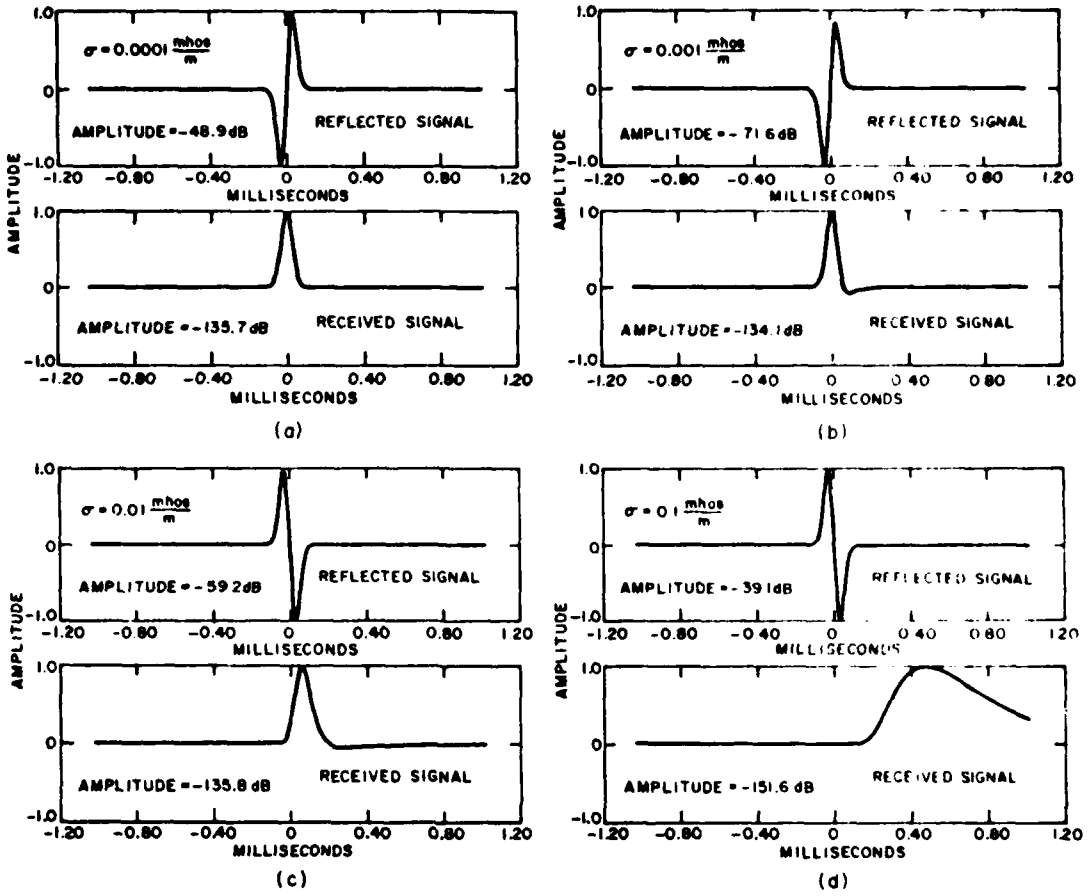

Figure 19. Signals reflected back into the transmission line from the input terminals of a 10m long dipole transmitting antenna and signals received on a 10m long dipole receiving antenna spaced 240m from the transmitting antenna. The dipoles are parallel and the input signal is a 0.1ms, 1 volt gaussian pulse. ε_r=4. Results are shown for four different conductivities: 10^{-4}, 10^{-3}, 10^{-2} and 10^{-1} mhos/meter. The source and load impedances used for the different conductivities are 4337 ohms, 433.8 ohms, 43.4 ohms and 4.3 ohms respectively. The amplitudes are in dB referred to the input pulse amplitude.

This attenuation factor can then be applied with very small error to any shape of input signal which is bandlimited within the LFW since transmission is effectively distortionless for such signals.

The received pulse shape shown in Figure 19(d) is remarkably similar to that obtained if a 1 millisecond pulse had been transmitted. The major effect is that the higher frequency energy contained in the 0.1 millisecond pulse has been highly attenuated. The concept of an attentuation factor is still valid because a distinct pulse having a clearly defined maximum is received. The difference is that a significant amount of high frequency energy has been attenuated and hence distortion has occurred during transmission. This is an important concept and will be discussed further in the following subsection.

The amplitudes of the reflected signals from the dipole increase as the conductivity increases from 10^{-3} mhos/m in Figure 19(b) to 10^{-1} mhos/m in Figure 19(d). This occurs because the relative dipole reactance increases with increasing conductivity (see Figure 7) thereby disturbing the reflection free match. In Figure 19(a) the reflected signal is larger in amplitude because the antenna reactance is negative and larger than when the conductivity is 10^{-3} mhos/meter.

Figure 20 is a plot of the attenuation factor A computed for the gaussian input pulse t_p=0.1 ms. The results presented in these plots are valid for signals band-limited at 10 KHz. They can also be used for signals whose bandwidth exceeds 10 KHz, as will be explained later.

There are several important and interesting features displayed in these graphs. First, the signal received is not strongly dependent on conductivity provided the input signal spectrum is within the LFW. The variation in received signal amplitude as the conductivity is changed by many orders of magnitude is within 3 dB, and these small differences have been ignored in the preparation of Figure 20. This result is rather surprising and needs further explanation. First, observe from Figures 7-9 that the dipole resistance for frequencies within the LFW is inversely proportional to the conductivity. This means that for a fixed input voltage the current on the dipole is proportional to the conductivity. The input voltage at our antenna terminals is fixed because the input impedance is constant and Z_s has been chosen to equal the input impedance. Because of our assumption of a fixed input voltage, Equation (9) shows that the electric field intensity of the element at zero frequency is independent of σ.

Equation (10) (shown plotted in Figures 2-5) shows that at low frequencies the conductivity has little effect on the amplitude of the electric field, and only changes the frequency scale of the frequency response curve. This characteristic is displayed in the curves shown in Figure 18. Thus the signal received is almost independent of conductivity when the input signal spectrum is within the LFW: the small differences are caused by the relationship of the input pulse spectrum (constant for the computations shown in Figure 19) to the

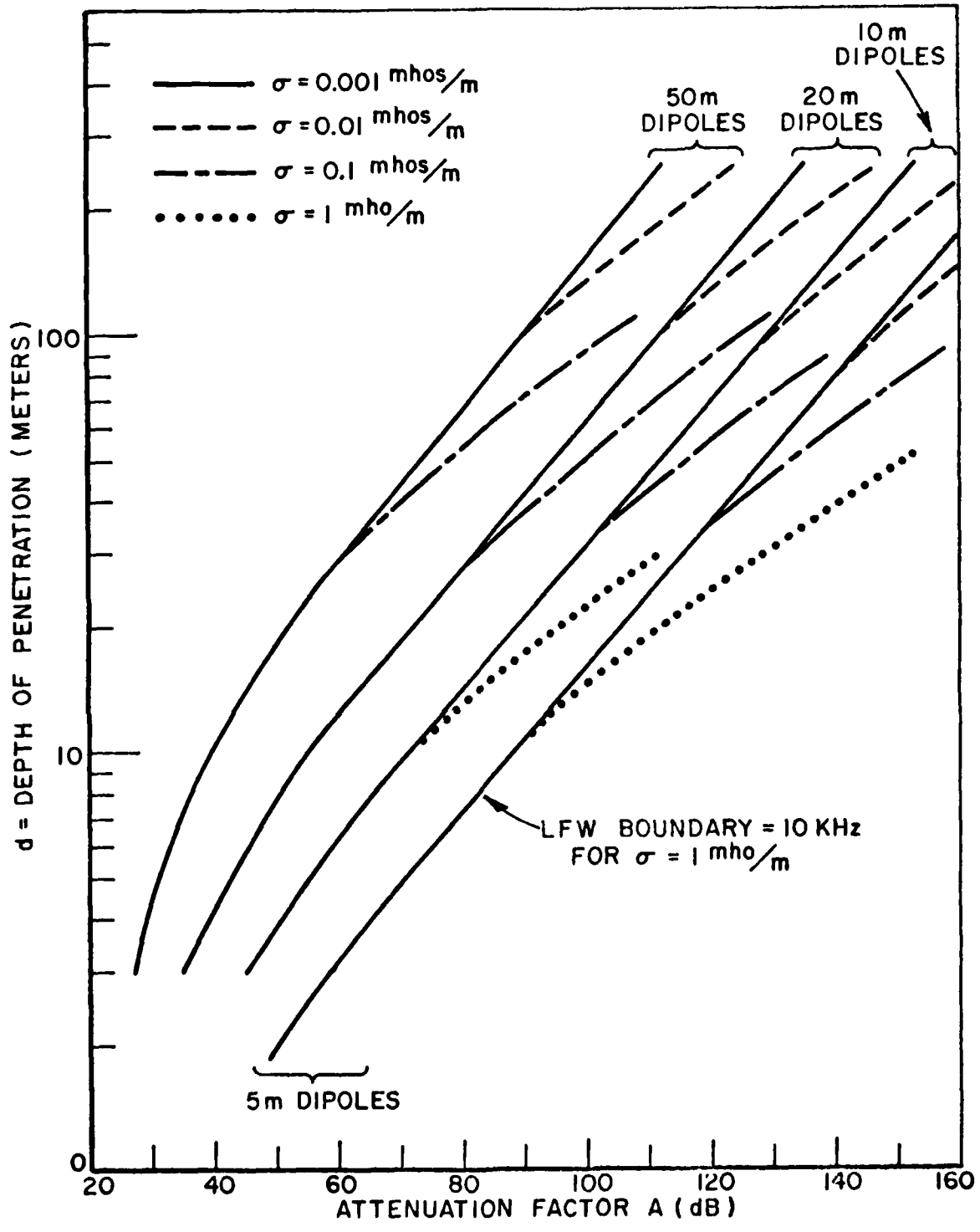

Figure 20. LFW radar attenuation factor curves for 5m, 10m, 20m and 50m dipoles. The data was computed for a 100 μs gaussian input pulse which is bandlimited at about 10 KHz. The LFW break-points therefore are for a frequency of 10 KHz.

shape of the transmission response of the medium, which changes slightly with conductivity, as shown in Figure 18. The major assumption then is that the pulse generator voltage is fixed. This assumption is justified because in a practical underground LFW radar the pulse generator voltage will be fixed by the voltage stored on the capacitors. A minor additional effect is that as the conductivity increases the antenna becomes electrically longer at a particular frequency. The resultant increase in the directivity increases the signal slightly over that caused by the mechanism discussed above, but we have not been able to isolate its effect.

The presentation of data for different source and load impedances in one graph, as is done in Figure 20, is justified since in a practical underground LFW radar the pulse generator and source impedance can be set by proper design to be the value required for the reflection free match, providing this value is not much smaller than one ohm. As a result, the data computed is presented in a practical form, and further, the data conveniently condenses into a set of universal design curves. Figure 20 is an example of such universal design curves.

The second feature to notice in Figure 20 is that A increases at a rate of 17 dB/octave of antenna spacing, providing the spectrum of the signal is within the LFW. When the signal spectrum exceeds the LFW, A increases significantly because of the energy lost in the low pass filtering action of the medium. The attenuation characteristic then departs from the straight line characteristic of the universal curves. The break points occur when twice the depth of penetration equals r in Equation (11) and f_m becomes less than the highest frequency contained in the transmitted pulse. Notice also that there is a slope discontinuity when the depth of penetration equals the antenna half-length ℓ. This is attributed to near-zone effects.

The third feature of interest is that increasing the length of the antenna two times decreases the attenuation by 17 dB.

The straight line characteristics suggest the following empirical formula for the attenuation factor.

$$\begin{aligned} \text{Attenuation factor} &= 17 \log_2 d - 17 \log_2(2\ell) + 73 \\ \text{(decibels)} \quad &= 56.5 \log_{10} d - 56.5 \log_{10}(2\ell) + 73 \qquad (27) \\ &\ell < d < 970/\sqrt{\sigma f_m} \end{aligned}$$

where the value 73 has been empirically elected to obtain a fit to the curves of Figure 20. In Equation (27) the radar range d and the antenna halflength ℓ are in meters, σ is in mhos/meter, and f_m is in Hz. Equation (27) is applicable for a wide range of conditions. However one condition is known where Equation (27) breaks down. This occurs when the antenna is long and the conductivity of the medium is high, so that the shunting effect of the conducting ground prevents current flow to the ends of the

antenna thereby reducing the effective length of the antenna. For long antennas the resistance of the conducting metal from which the antenna is made can have a noticeable effect on the attenuation factor: however we have only noticed this effect when the antenna length exceeds about a kilometer. A conservative formula for this constraint on (27), based on the results of calculations made on very long antennas, is

$$f_m \sigma \ell < 500 \text{ ohm}^{-1} \text{ sec}^{-1} . \qquad (28)$$

The parameters for the calculations presented in this report fall within the bounds of (28).

When the straight line characteristics of Figure 20 are used to determine the attenuation factor, the result so obtained has been shown by other computations often to be valid for signals having bandwidths considerably greater than 10 KHz, because the LFW boundary varies with range (although the curved sections of the characteristics are only valid for 10 KHz bandlimited signals). For example if σ=.001 mhos/m, d=50 m and 2ℓ=20 m, Figure 20 gives A= 94 dB. This result could be used to f_m=376 KHz according to (11) with r=2d. This would depend upon the input impedance of the antenna remaining largely resistive up to that frequency, and a computation would need to be done to verify this. However for 2ℓ= 10 m, d=9.7 m and σ=1 mho/m, f_m=10 KHz as illustrated in Figure 20.

It should be noted that the results just presented are for the antenna *in an infinite conducting medium.* When the antenna is near the earth's surface there is only one half space of conducting earth to load the antenna: This makes the design constant used in (27) even more conservative because the amount of loading caused by the lossy ground on the signals traveling along the antenna, from which the constant in Equation (27) was determined, is reduced.

(2) Considerations in a Practical Radar Design

In Figure 19 it is observed that there is insufficient range delay time to separate the transmitted pulse and the received signal except for the case when σ=0.1 mhos/m. This means that the only transmit-receive isolation possible is that obtained from the decoupling of the transmitting and receiving antennas. It is very desirable to have the transmitted signal and the received signal time separated so that the received signal can never be confused with direct coupling of the transmitted signal to the receiver.

Figure 19(d) suggests that to obtain sufficient range delay of the received signal the input signal should contain energy at frequencies higher than the LFW cutoff for a given system. The energy above the LFW cutoff is heavily attenuated by the medium and hence does not contribute to the received signal. However the energy is present on the transmitting antenna, and serves to sharpen the transmitted pulse so that good range

separation is obtained. The penalty is an increased attenuation so that a compromise between range separation and attenuation factor is necessary. A suitable compromise is to increase the bandwidth of the input pulse to 10 times the LFW cutoff which results in an increase in the attenuation factor by 10-15 dB.

Figure 21 shows the relative locations of the received signal and

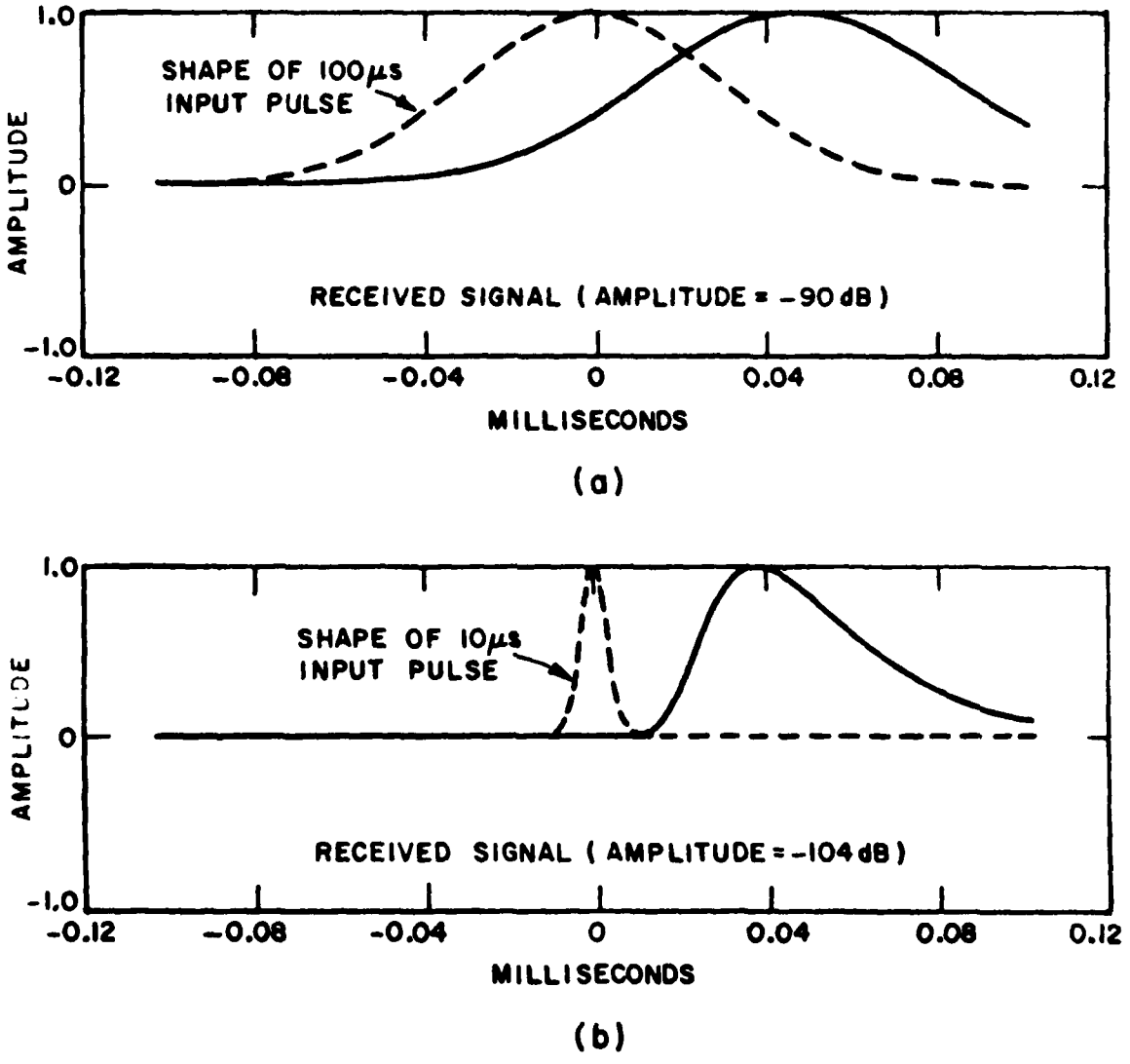

Figure 21. Relative locations of received signal and (a) 100 μs input pulse and (b) 10 μs gaussian input pulse for 50m dipoles spaced 2d=200m in a medium of ε_r=4 and σ=.01 mhos/m.

the input signal for 50 m dipoles spaced 200 m in a medium of ε_r=4 and σ=0.01 mhos/m. Two input signals are shown, one is a 100 μs pulse which is approximately bandlimited at 10 KHz, which is the LFW cutoff for the system, and the other is a 10 μs pulse which contains significant energy to about 100 KHz. It is seen that for the shorter input pulse the range delay is sufficient to separate the transmitted and received signals. The penalty is an increase in attenuation of 14 dB. The isolation between the transmitting and receiving antennas could be up to 100 dB if a well designed orthogonal antenna system is used (Burrell and Peters, 1976). However it is desirable to have a total isolation of greater than 120 dB for a successful design (this is a figure arrived at by considering possible input pulse amplitudes and receiver sensitivities, and rather than being a fixed design parameter it is a guideline). For the case illustrated in Figure 21(b) the signal coupled directly from the transmit antenna to the receive antenna would occur at the location of the input signal, and be 4 dB greater in amplitude than the received signal. However because of the range separation obtained by implementing the procedure outlined above, the received signal is readily detectable.

It is observed that in Figure 20 the shapes of the curves for each conductivity when the LFW is exceeded are approximately straight lines with a slope of 26 dB/octave. Therefore an attenuation curve can be constructed for any pulse length and conductivity simply by calculating the radar range at which the LFW cutoff frequency equals the highest significant frequency in the pulse, and drawing a line of slope equal to 26 dB/octave to intersect the attenuation curve constructed from Equation (27) at that range. Figure 22 is an example of a curve constructed in this way for a medium conductivity of 0.03 mhos/m and an input pulse duration of 200 μs. This pulse is approximately bandlimited at 5 KHz, and the LFW cutoff equals 5 KHz when d=79 m. Accordingly Figure 22 was constructed. The result of a sample calculation is also included, and the simple graphical method is seen to give good accuracy.

By using Figure 20 and the graphical procedure, and the assumption that the input pulse should contain frequencies in excess of the LFW cutoff to increase the attenuation factor by 10 dB, Table 1 has been constructed. This table gives the maximum range of an LFW radar operating in ground of different conductivities, and is based solely on consideration of the input signal spectrum. The attenuation factors for different antenna lengths are included. It is noted that some of these figures are high (as discussed earlier, a practical radar will probably operate with an attenuation factor of about 100 dB) and in practice the maximum range given by Table 1 may not be achieved because of constraints on the input signal amplitude, the receiver sensitivity, or clutter level. Conversely it is noted that for a 20 m antenna and σ=1 mho/m A is only 81 dB. In this case the maximum range may be increased beyond 25 meters if the radar design permits additional attenuation. The benefit obtained in this case is an increased range window.

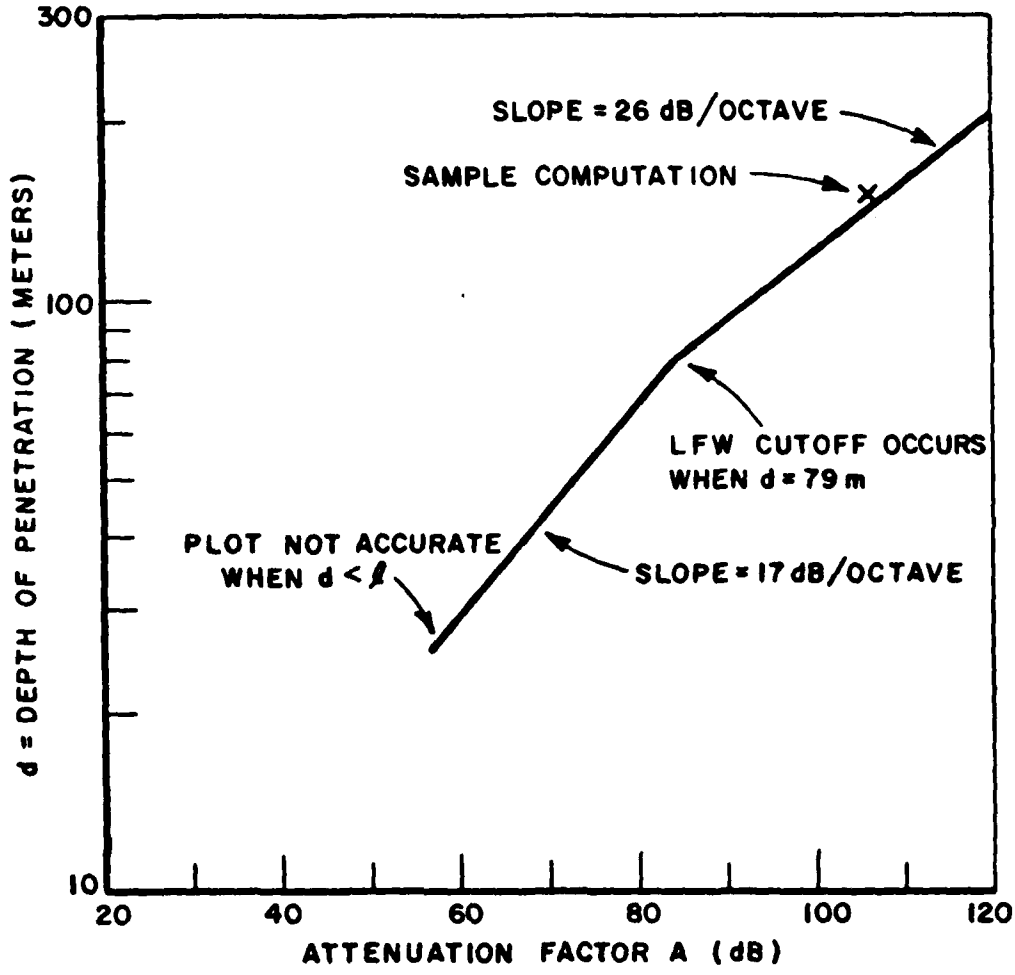

Figure 22. Example of attenuation curve constructed for σ=0.03 mhos/m and input pulse of 200 μs duration using graphical procedure. A sample computation indicates that the curve so constructed is accurate to 2 dB. The antenna length 2ℓ=50m.

TABLE 1

MAXIMUM RANGE OF LFW RADAR DETERMINED FROM CONSIDERATION OF THE INPUT SIGNAL BANDWIDTH

σ (mhos/m)	Maximum range d (meters)	Attenuation factor A (dB) for given dipole length			
		5m	10m	20m	50m
1	25	120	104	81	-
0.1	75	148	130	115	92
0.01	220	-	158	140	118
0.001	650	-	0	169	147

8. PULSE PROPAGATION IN THE HFW

For propagation in the HFW, the transmission transfer function for parallel non-displaced dipoles is no longer almost constant as it was in the LFW. Consequently there is significant distortion of the input pulse. In particular, because insulated antennas will inevitably be used for HFW radars, there is effectively no transmission at low frequencies, and the received signal will have no average (d.c.) value. To obtain efficient transmission in the HFW when using dipole type antennas it is necessary to choose the antenna length so that antenna resonance occurs in the frequency band of operation of the radar. A design goal is to minimize this resonance so that the antenna has a wide bandwidth, but it is still expected that the same constraints on the length of the antenna will exist. Improvements in the antenna design are beyond the intent of this report; only propagation between simple dipoles considered here. Antenna design will be treated further in a later report.

There are several advantages in operating a radar in the HFW. Among these are

1) The antenna is portable because it does not have to be in conducting contact with the ground, and it is considerably smaller in general than a LFW radar antenna.

2) The band of frequencies which can be transmitted is often many decades of frequency higher than that passed by the LFW. This means that short input pulses can be used, and a much wider separation in time is obtained between the transmitted and received signals (called a clear range window). This clear range window means that it is possible from a signal separation viewpoint to use the same antenna for transmitting and receiving.

3) High frequency scattering information means that identification of targets whose characteristic dimensions are of the order of one or two meter radius tunnels is feasible.

The concept of an attenuation factor has been retained in this section in spite of the received signal not, in general, being a near replica of the input signal. Its usefulness is that it relates the peak amplitudes of the transmitted and received signals. The transmitted signal will usually be a simple signal such as a pulse or doublet, and is readily described by its peak amplitude. The peak value of the received signal is useful as a measure of the "visibility" of the signal to the receiver.

In Section 2 it was shown that for propagation to be practical in the HFW the dip in the frequency response curve for the elemental dipole should be less than about 10 dB. In Section 5 it was shown that if the radar antennas are insulated then the frequency band of operation of the radar should be on the part of the curve where the electric field slopes upward at 6 dB/octave of frequency. If this is not done then significant signal loss will occur because the conduction currents are not strongly excited when the dipole is insulated (Figure 12). As discussed in Section 2, the upward sloping part of the frequency response curve occurs when α is constant. Hence we conclude that an HFW radar should operate in a frequency band where α is constant. The lower limit of this band can be determined from Figure 1. It should be noted that operation of a radar through the transition region (where α and β are given by (2) and (3)) is possible providing the antennas are not insulated. However operation at higher frequencies with insulated antennas seems more desirable and consequently the transition region will not be further considered here.

Design Curves for HFW Radars

When α is constant over the frequency band of operation of the radar, the attenuation factor A (which relates peak amplitudes of signals) can be written as

$$A = A_o \frac{e^{-2\alpha d}}{2d} \quad . \tag{29}$$

A_o is a constant which is determined by numerical experiment for a particular antenna geometry, medium, generator impedance and input signal. The factor $e^{-2\alpha d}$ accounts for the medium attenuation over the distance 2d, and the 2d in the denominator accounts for the signal loss due to spatial attenuation (or the spherical expansion) of the fields of the dipole. The only effect of α is to introduce signal attenuation.

Figure 23 shows the system responses for two 1 m long dipoles separated by 2d = 60 m in a homogeneous medium of σ=0.001 mhos/m and ϵ_r=9. The dipole radii were 0.001 m and each were coated with a 0.0015 m radius layer of polythene (ϵ_r=2.3). The upper plots are $\rho(f)$ and H(f),

and the lower plots show the signal reflected from the terminals of the transmitting antenna and the signal observed on the receiving antenna when a 5 ns gaussian pulse is transmitted. The source and load impedances were set at 200 ohms. Note that the transmission coefficient plot H(f) shows that significant energy is transmitted when the antenna is about a half wavelength long in the medium (≈100 MHz). Significant energy is also transmitted when the antenna is about 1.5λ long (300 MHz), but the transmission efficiency is less than that for the first resonance because the effective length of the receiving antenna when it is 1.5 wavelengths long is about a third the effective length when it is 0.5 wavelengths long. Little energy is transmitted when the antenna is 1 wavelength long because its input impedance is high.

The peak received signal is 92.5 dB below the transmitted signal, i.e., A is equal to 92.5 dB. Observe also that the scale is shifted for the received voltage waveform and that it is delayed by a time corresponding to approximately 100 transmitted pulse widths, so that there is a very clear range window. It should be practical to observe the reflected signal on the transmit antenna if there are no reflections from parallel layers present.

Figure 24 shows the same antenna system but 2d=30 m. Note that the shape of the received signal is identical to that shown in Figure 23, but the amplitude has changed by 22.1 dB. Figure 25 shows computed values for A for this medium and also for a medium of σ=0.005 mhos/m and ε_r=16. The excellent agreement with the best fit curves of the shape exp (-2αd)/2d confirms Equation (29).

Equation (29) can be expressed in decibels

$$A(dB) = A_1(dB) + A_F(dB), \tag{30}$$

where A_F is given by

$$A_F(dB) = 20 \log_{10} \left(\frac{e^{-2\alpha(d-1)}}{d} \right) \tag{31}$$

and the constant A_1 is given by

$$A_1(dB) = 20 \log_{10}(A_o) \tag{32}$$

where A_o is the value taken for d=1 meter. A_F is the medium attenuation function and is normalized to have unit value when d = 1 meter. Figure 26 is a plot of A_F for media having different values of α. Table 2 shows the high frequency forms for α for a wide range of media constitutive parameters. Figure 1 is useful as a gauge of the frequency at which α reaches its high frequency asymptotic form.

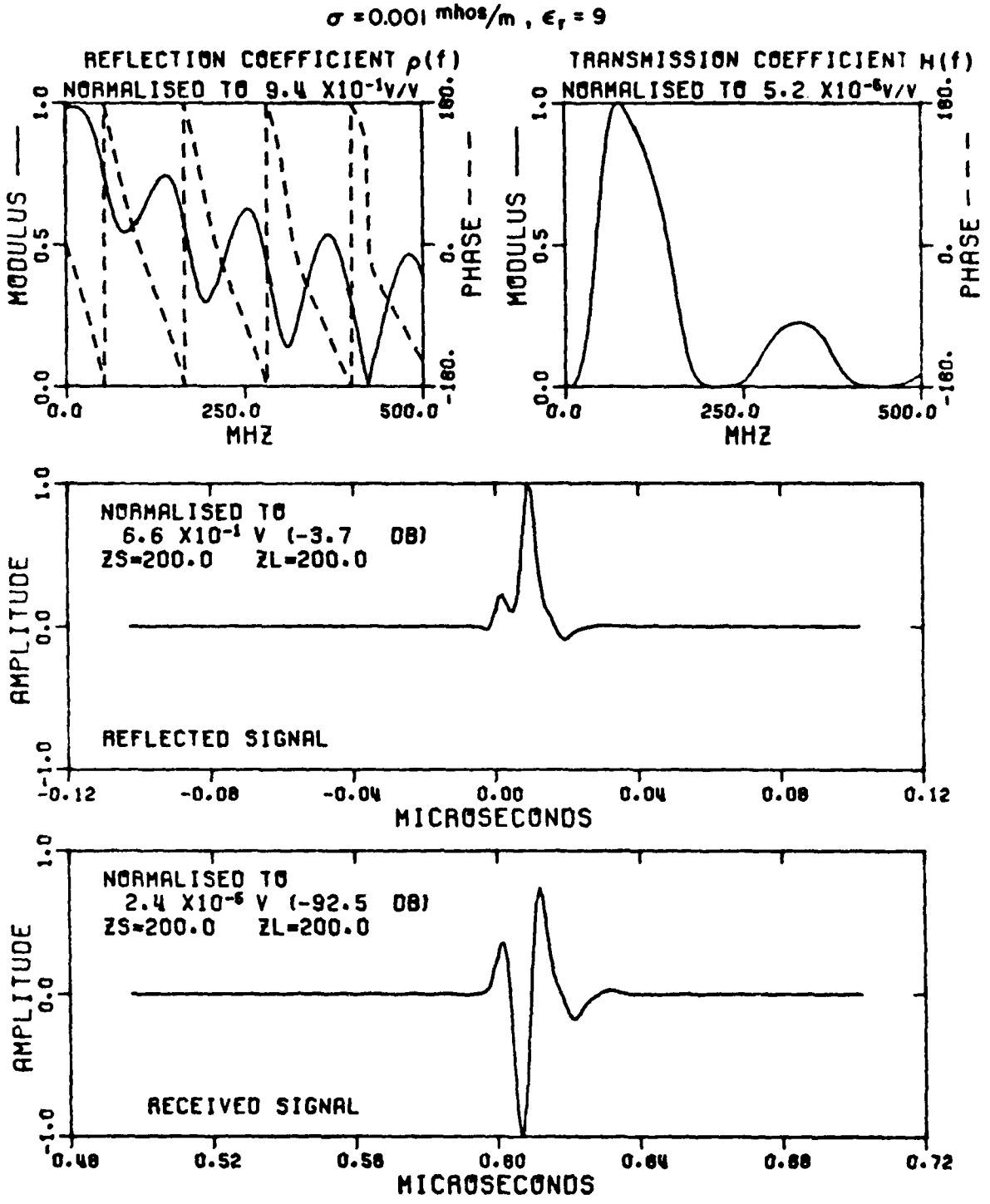

Figure 23. System responses for two 1 m long, 0.001 m radius dipoles separated by 2d=60m in a homogeneous medium of σ=.001 mhos/m and ε_r=9. The dipoles are coated with a 0.0015m radius layer of polythene insulation (ε_r=2.3). The upper plots are the system frequency responses. The lower plots are the signals obtained when the frequency responses are weighted by the spectrum of the input signal and transformed into the time domain. The input signal was a 5 μs gaussian pulse.

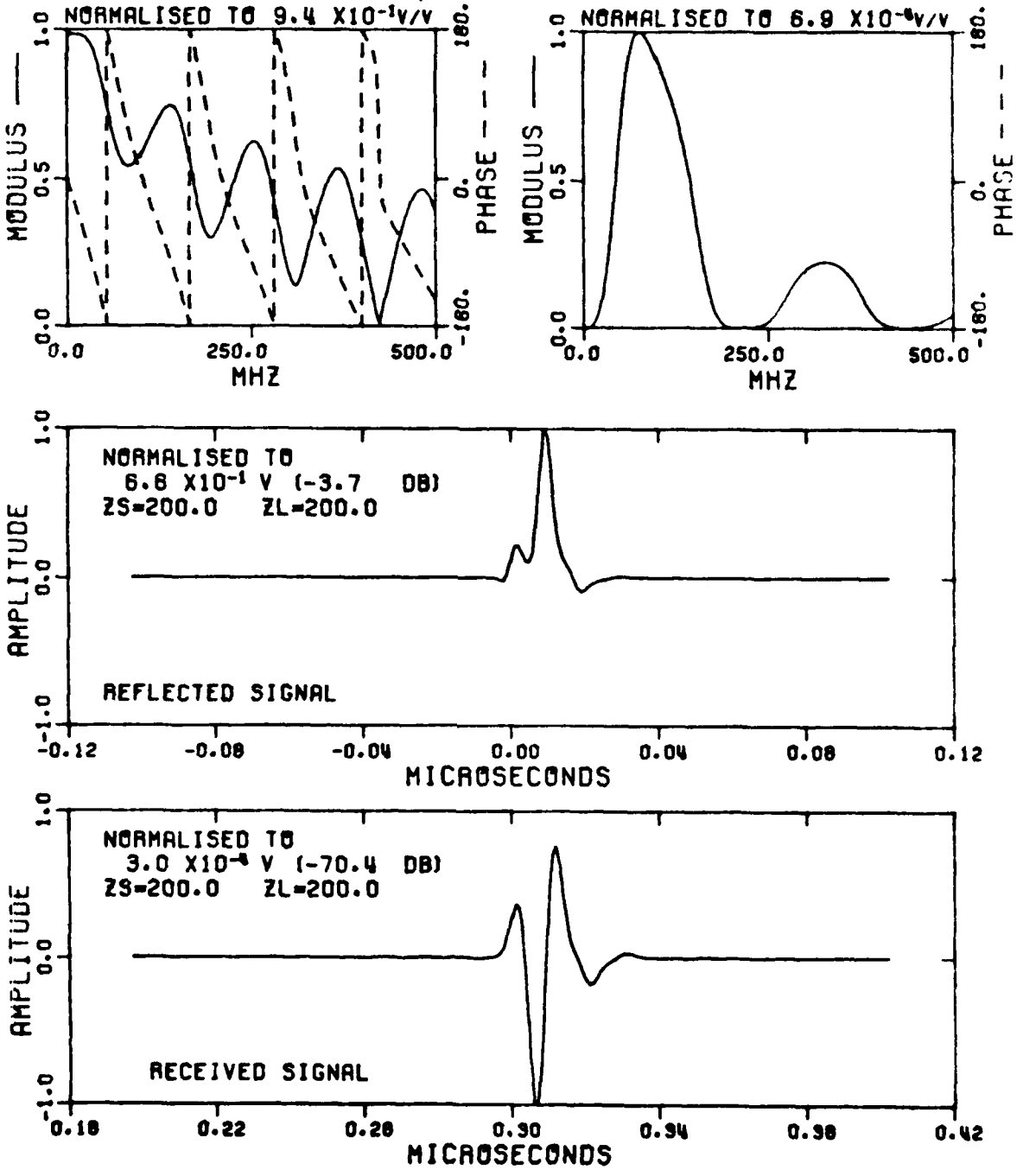

Figure 24. System responses for same geometry as Figure 23 but 2d=30m.

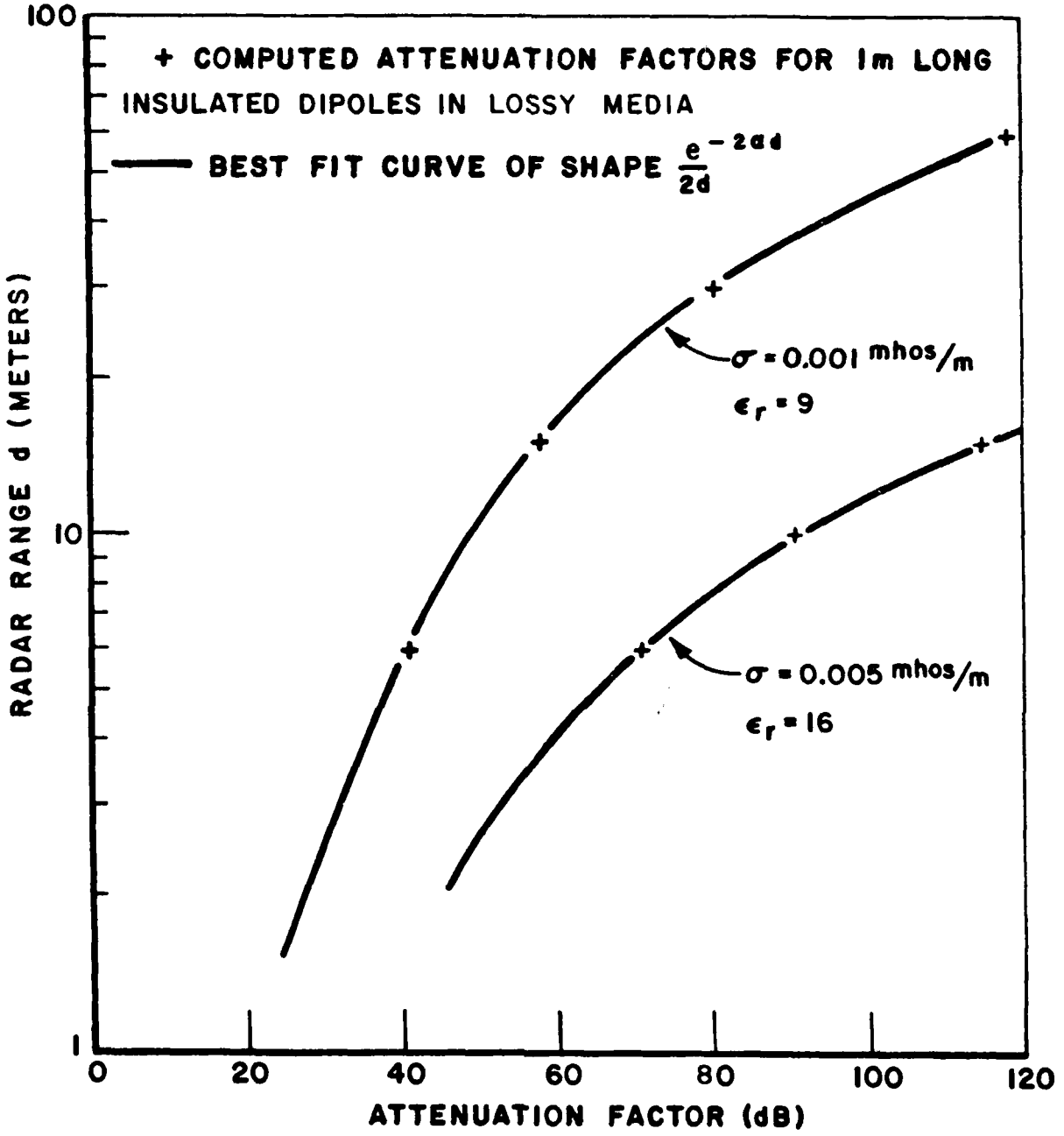

Figure 25. Attenuation factors for 1 m long, 0.001 m radius insulated dipoles computed for two different media with best fit curves.

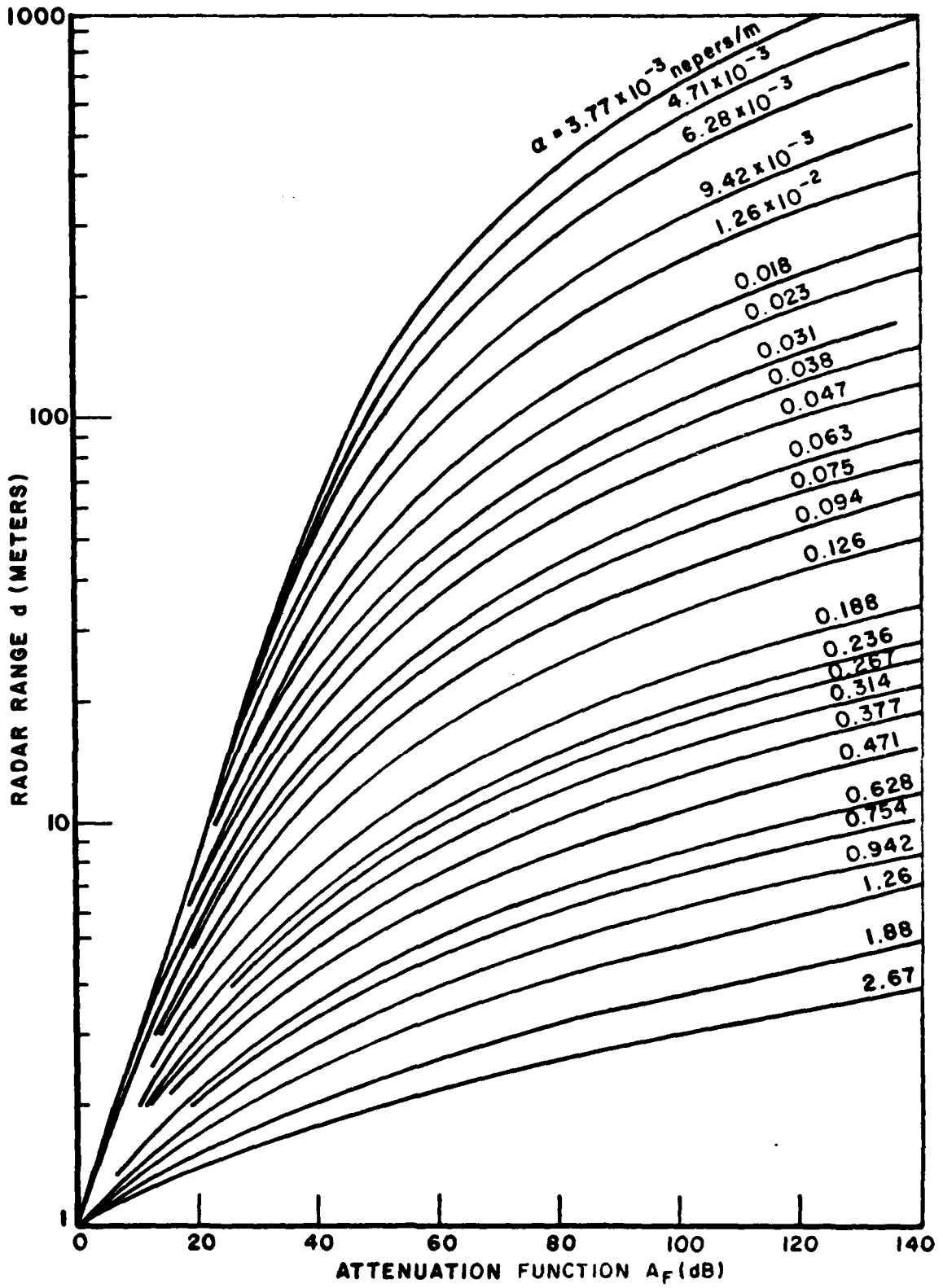

Figure 26. HFW radar medium attenuation functions for selected high frequency asymptotic values of α.

TABLE 2

HIGH FREQUENCY ASYMPTOTES FOR α (NEPERS/M)

σ mhos/m / ε_r	.0001	.0002	.0005	.001	.002	.005	.01	.02
2	1.333×10^{-2}	2.666×10^{-2}	0.067	0.133	0.267	0.666	1.33	2.67
4	9.42×10^{-3}	1.88×10^{-2}	0.047	0.094	0.188	0.471	0.942	1.88
9	6.28×10^{-3}	1.26×10^{-2}	0.031	0.063	0.126	0.314	0.628	1.26
16	4.71×10^{-3}	9.42×10^{-3}	0.023	0.047	0.094	0.236	0.471	0.942
25	3.77×10^{-3}	7.54×10^{-3}	0.018	0.038	0.075	0.188	0.377	0.754

The constant A_1 is a function of antenna length, antenna type, medium constitutive parameters, generator source impedance (and receiver load impedance), and input signal. In this report we have restricted ourselves to the simple dipole, and we have further reduced the number of data required by choosing a 1 meter long antenna (it will be shown later that antenna length can be simply accounted for).

The choice of a generator source impedance and an input signal required considerable deliberation. The input impedance of the straight, insulated dipole is not constant over a wide frequency range. One essential choice of generator source impedance is a constant resistance, because this best simulates the transmission lines which will inevitably be used to feed HFW radar antennas. The value selected was 200 ohms, which satisfied two criteria. The first is that it is physically realizable as a balanced transmission line made by connecting two pieces of 100 ohm coaxial cable in series. The second criterion is that 200 ohms approximately matches the surge impedance of a dipole antenna so that the reflection of the input pulse from the terminal region of the dipole is relatively small (observe that in Figures 23 and 24 the first peak in the reflected signal, which is the pulse reflected from the terminals, is about -18 dB of the input signal amplitude). It has been further observed that the level of the received signal is not significantly affected by relatively large changes in the source resistance (little change was observed as Z_S varied from 50 ohms to 200 ohms).

The choice of a constant resistance for the generator source impedance does not give a reflection free match nor maximum power transfer (see Section 4). Because we are constructing our signals from data tabulated at many frequencies, we can choose different matching impedances at different frequencies. These could correspond to some physically realizable network, or they could just as easily represent a non physical network. If a reflection free match, Equation (17), is modelled, then a network could be constructed which would have a frequency response similar to that of the dipole. However a network to provide a conjugate match over a wide frequency band is not physically realizable. The conjugate match does however give the maximum power transfer, and therefore gives the best power transfer which can be obtained by antenna matching. For this reason we chose also to investigate the transmission when a conjugate match is used. In this case we chose the input signal in a special way, as will be shown later. It is pointed out that the conjugate match data would be applicable if pulse signals were ever reconstructed from a set of c.w. measurements, because in this case a conjugate match could be obtained for each frequency measurement. It may also be possible to adjust the phases of the frequency components of the received signal (assuming a reasonable estimate of the ground parameters is available) to maximize the visibility of the wanted signal in the noise.

Several choices of input signal were possible. The simplest input signal to generate in practice is a single pulse similar in shape to the gaussian pulse used for the LFW calculations. We chose a gaussian as one of our input pulses.

Inspection of the transmission coefficient in Figures 23 and 24 shows that little energy is transmitted at low frequencies which is where the simple gaussian pulse has most of its energy concentrated. We would expect less transmission loss if we "tailored" the input signal so that its spectrum more closely matched the shape of the transmission coefficient of the system consisting of the antennas and the medium. Because there is effectively no transmission at zero frequency, such an input signal should have no average value. A gaussian doublet was chosen.

There are two ways of generating a gaussian doublet. The first is simply to differentiate Equation (25) to obtain

$$u(t) = \frac{-11t}{t_p^2} \; e^{-5.5t^2/t_p^2} \tag{33}$$

This signal can be generated by a differentiating network (Burrell, 1971, Ch. 4) but the output level of the differentiating network is often low. The spectrum of this signal is the spectrum of the gaussian pulse (Figure 19) multiplied by $\omega=2\pi f$. Therefore there are no zeros in the spectrum of Equation (33).

The second way to generate a doublet is to add two gaussian pulses, one of which is inverted and displaced in time with respect to the other. Such a signal can be generated by a simple transmission line network (Ross, 1965), and good output levels obtained. We chose this method, and the signal used was

$$u(t) = e^{-5.5(t+t_s)^2/t_p^2} - e^{-5.5(t-t_s)^2/t_p^2} \tag{34}$$

where

$$t_s = 0.7\ t_p\ . \tag{35}$$

An example of this gaussian doublet and its spectrum are shown in Figure 27.

Finally, we chose a third input signal. We have obtained maximum power transfer by using a conjugate impedance match for one of our methods of matching. The strongest peak output signal is obtained by using as the input signal a transient whose spectrum equals the complex conjugate of the system transfer function. So, for the conjugate match we chose the optimum input signal in this way. It is emphasized that although the match is non-physical, the input signal is physically realizable, although it may be difficult to generate in practice.

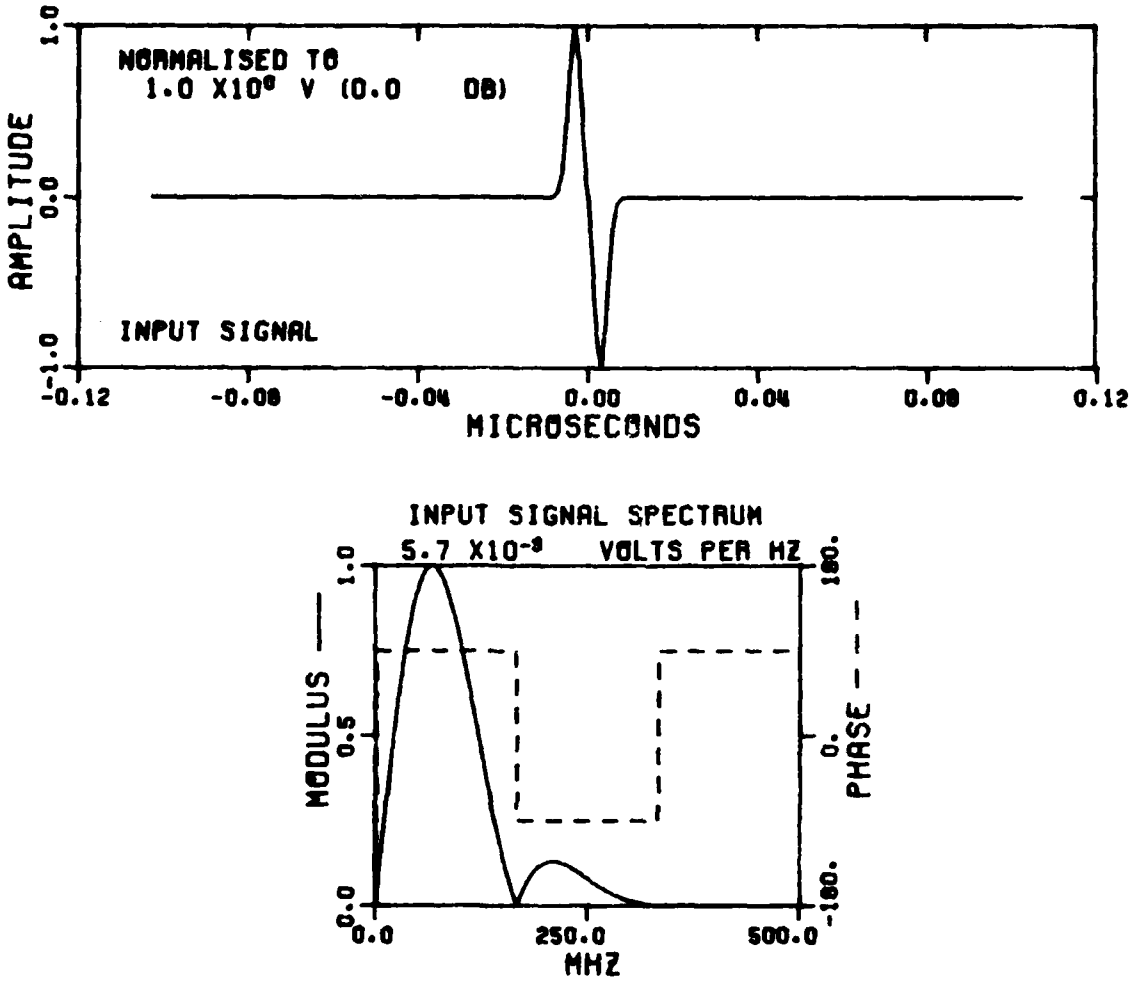

Figure 27. 10 ns gaussian doublet input signal (t_p=5 ns).

The use of an input signal optimized in this way, together with a conjugate match, gives a received signal which can be compared with those obtained using the practical matches and generators to gain an idea of how much signal is being lost due to poor impedance matching and less than optimum input pulses.

Table 3 shows values of A_1 for the three cases discussed for a range of input signals. Note that the signal improvement obtained by using an optimum input signal and a conjugate match is generally 20-30 dB, and that the signal improvement obtained by using the gaussian doublet instead of the simple pulse is about 4 dB.

Observe that for the optimum case, there is an occasional negative entry in the table. This corresponds to a gain over the planar wave propagation factor and involves a very carefully designed pulse plus a possible non-realizable impedance to achieve the optimum match.

TABLE 3

VALUES FOR CONSTANT A_1 FOR 1 m LONG INSULATED DIPOLES IN LOSSY MEDIA. THE DIPOLE RADIUS IS 0.001 m AND THE OUTER RADIUS OF THE POLYTHENE INSULATION (ϵ_r=2.3) IS 0.0015 m. FOR THE OPTIMUM INPUT SIGNAL A CONJUGATE MATCH WAS USED: FOR THE OTHER INPUT SIGNALS A 200 OHM MATCH WAS USED.

ϵ_r	σ (mhos/m) Input Signal	.0002	.0005	.001	.002	.005
2	optimum	2.2 dB	11.8 dB	19.9 dB	-	-
	5 ns pulse	34.3 dB	34.7 dB	37.8 dB		
	8 ns doublet	28.4 dB	28.1 dB			
4	optimum	-3.6 dB	6.4 dB	14.2 dB	20.4 dB	-
	5 ns pulse	30.6 dB	31.1 dB	32.9 dB	34.5 dB	
	8 ns doublet	25.7 dB	26.4 dB	28.3 dB	31.2 dB	
9	optimum	-9.5 dB	0.5 dB	8.6 dB	16.2 dB	25.5 dB
	5 ns pulse	29.6 dB	30.3 dB	31.2 dB	32.8 dB	37.0 dB
	8 ns doublet	25.0 dB	25.7 dB	27.1 dB	28.3 dB	33.6 dB
16	optimum	-1.5 dB	-6.2 dB	2.3 dB	10.9 dB	20.3 dB
	5 ns pulse	37.7 dB	29.6 dB	31.2 dB	31.5 dB	33.5 dB
	8 ns doublet	30.8 dB	24.7 dB	26.3 dB	29.0 dB	29.2 dB
25	optimum	-17.3 dB	-9.0 dB	-2.9 dB	6.1 dB	-
	5 ns pulse	30.5 dB	30.9 dB	30.7 dB	31.8 dB	
	8 ns doublet	25.7 dB	26.1 dB	26.0 dB	27.2 dB	

Figure 28 shows the received and reflected signals for the case σ=0.001 mhos/m, ε_r=9 and d=30 m when the gaussian doublet input signal of Figure 27 is used. Figure 29 shows the system responses when a conjugate match is used and the reflected and received signals when the input signal is optimized. The optimum input signal for this example is shown in Figure 30. Note that the attenuation factor of 69.6 dB for this case is obtained by taking the difference of the received signal amplitude shown in Figure 29 and the optimum input signal shown in Figure 30.

In this section, the examples shown in Figures 23, 26, and Figures 28 and 29 are all for a conductivity of 0.001 mhos/m and ε_r=9. These illustrations in no way imply that the design data presented in this section is for these specific parameters, as Figures 25, 26 and 31 testify.

Target recognition is an important feature of underground radar. Information on the target resonances is required for recognition schemes which are based on complex resonances (Moffatt and Mains, 1975). The underground radar designer knows the type and approximate dimensions of the target, although there may be considerable uncertainty as to its precise electrical composition. In the case of tunnels however they are either flooded or airfilled, so that the electrical properties of the target are known. Further, the dimensions of man made tunnels (mine shafts, road tunnels, etc.) are known within an order of magnitude. Consequently the resonant frequencies of these targets can be predicted with reasonable accuracy, and the frequency band of operation of the radar selected accordingly. This determines the length of the dipoles. This topic will be discussed further in a forthcoming report.

Figure 31 shows how the attenuation factor depends upon the dipole length. Two examples with different ground parameters are shown. In the calculations used to prepare Figure 31 the frequency range of the data, the pulse duration and the antenna radius were scaled in proportion to the antenna length. For example, for the 4 m long antenna, data was collected to 125 MHz and a 20 ns gaussian input pulse was used. In each case a 200 ohm resistive match was used because this value is not dependent on the antenna length (unless it is very short) but is dependent on the surge impedance of the antenna.

Note that the attenuation factor reduced by about 6 dB for each octave increase in dipole length. Note that from Equation (36) in the following subsection a two times increase in the effective height of the dipole is offset by a halving of the frequency (contained in $\gamma=\alpha+j\beta$; $\beta>>\alpha$) so that the field radiated from the transmitting dipole is unchanged when both the frequency range and the antenna are scaled in the way described above. However the voltage induced on the receiving dipole is proportional to the effective height, so that doubling the antenna length results in a 6 dB improvement in signal level.

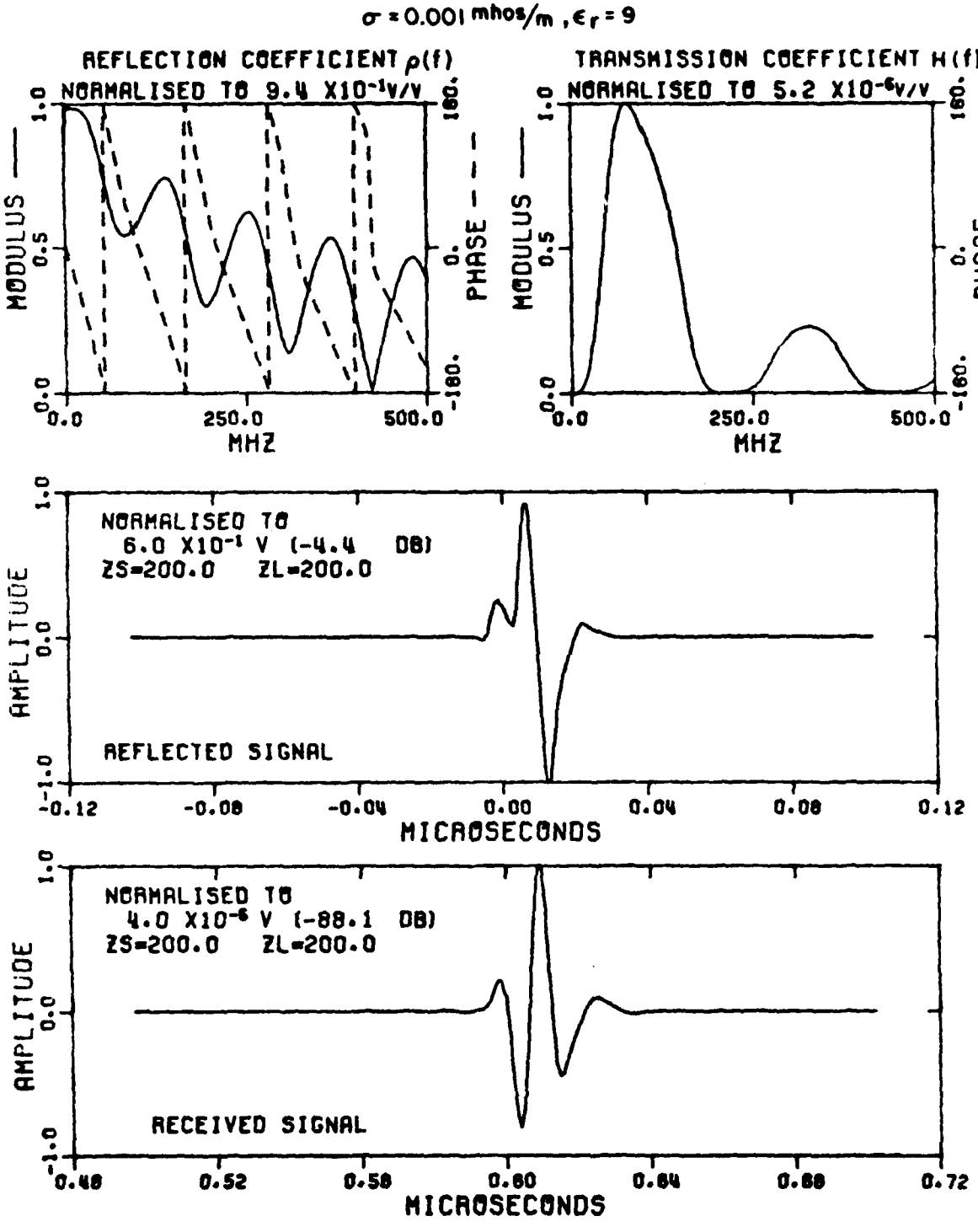

Figure 28. Responses for antenna system used in Figure 23, but with t_p=5 ns gaussian doublet input signal.

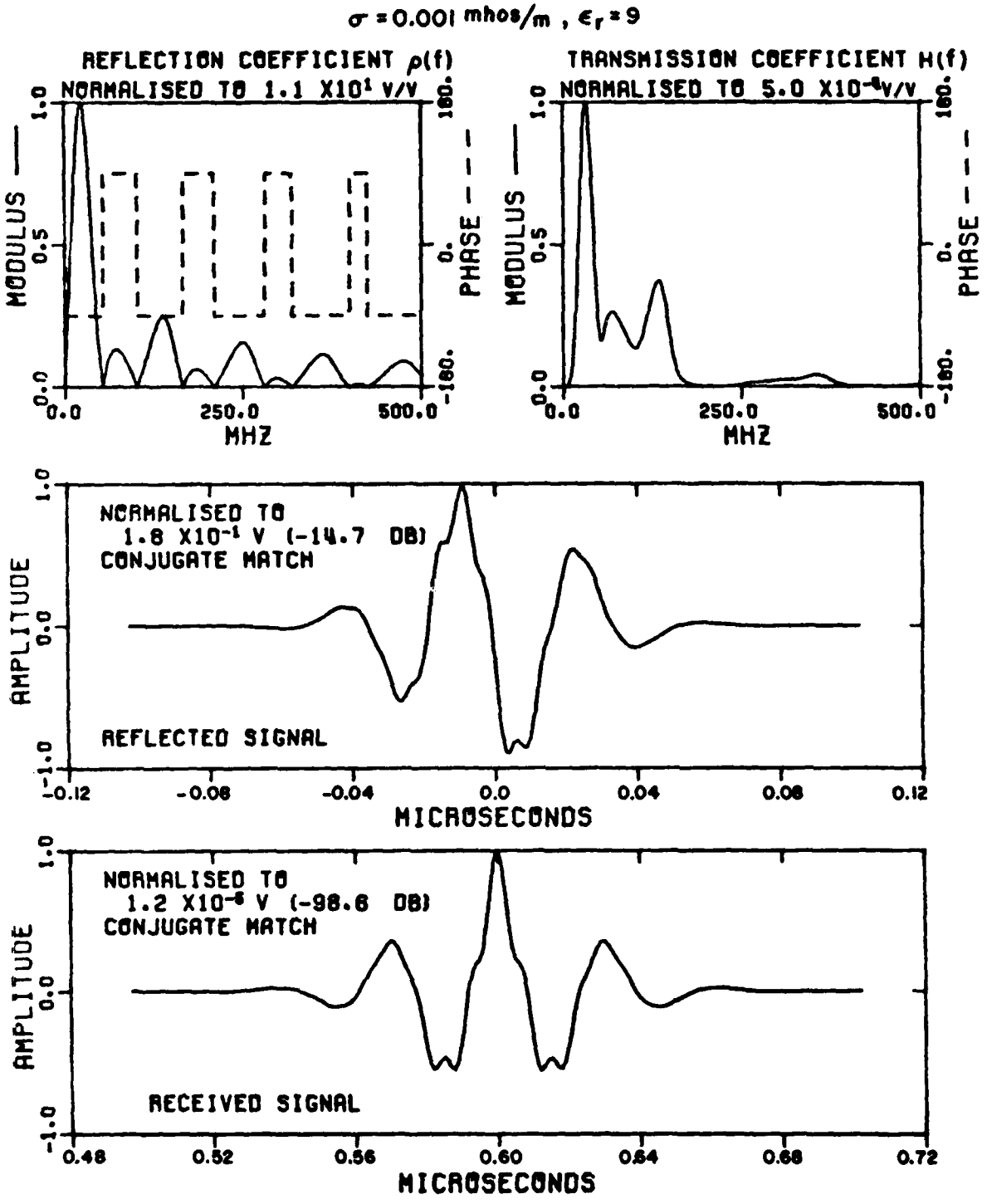

Figure 29. Response for antenna system used in Figure 23, but with a conjugate antenna match simulated for all frequencies and an optimum signal input. The optimum signal spectrum is chosen to be the complex conjugate of the transmission coefficient H(f).

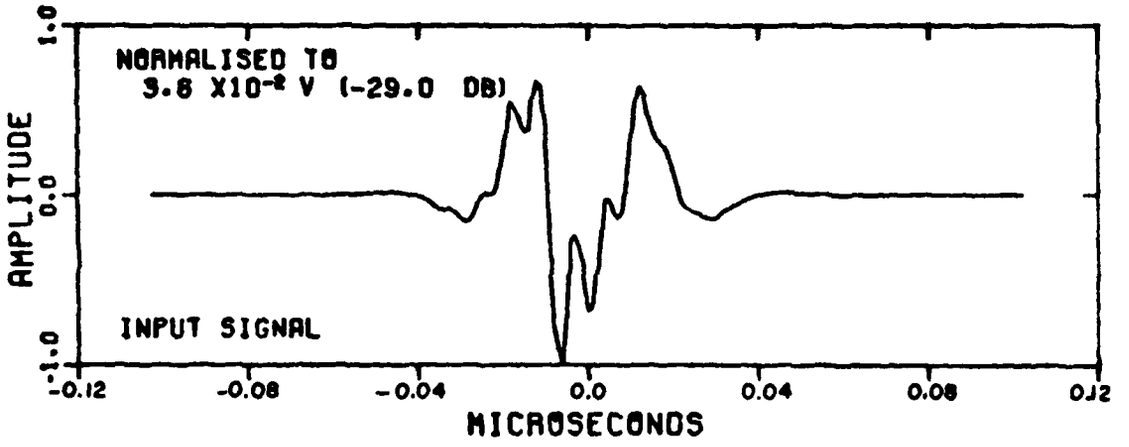

Figure 30. Optimum input signal used for example shown in Figure 29.

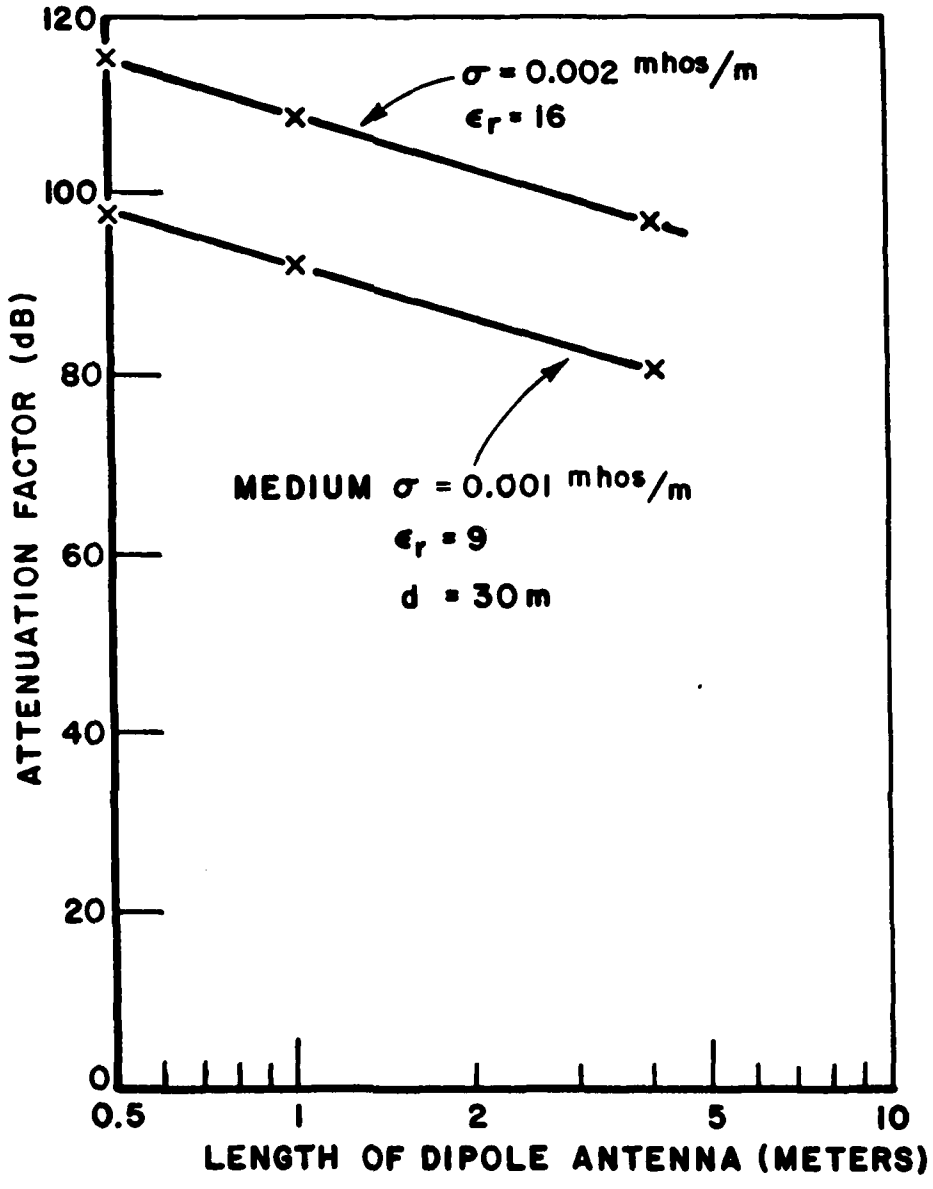

Figure 31. Illustrating the variation of attenuation factor with antenna length for HFW radars. The input signal duration is scaled together with the antenna length and radius.

Effective height calculations

The results presented in this section were obtained from z matrix computations using the model developed in Section 6. This procedure is exact for all frequency ranges and antenna spacings. When the two antennas are in their respective far fields so that Equation (29) applies, a more efficient computational procedure is to use the complex effective height.

The field radiated from a dipole is given by

$$E^{rad}(f) = \frac{\eta}{4\pi} \gamma h_e(f) I_o(f) \frac{e^{-\gamma r}}{r} \tag{36}$$

where η is the characteristic impedance of the medium, $I_o(f)$ is the terminal current on the dipole, and $h_e(f)$ is the complex effective height of the dipole in meters. The moment method program we used (and this is true with most moment method programs) had a 1 volt generator to drive the antenna, so

$$I_o(f) = \frac{1}{Z_{in}(f)} \tag{37}$$

and

$$h_e(f) = \frac{4\pi}{\eta\gamma} Z_{in}(f) \frac{r}{e^{-\gamma r}} E^{rad}(f). \tag{38}$$

$E^{rad}(f)$ is the far field at a distance r meters broadside to the dipole and would be computed using the moment method solution. $h_e(f)$ can then be used to find H(f) for the system of two dipoles which are in their respective far fields:

$$H(f) = \frac{\eta \gamma h_e(f)^2 Z_L}{2\pi[Z_s + Z_{in}(f)]} \tag{39}$$

The advantage of using Equation (39) is that because only one antenna is modelled the computer time is reduced by approximately a factor of 4.

9. USE OF THE PROPAGATION CHARTS

Design data has been presented for LFW radars and HFW radars. The choice of the radar to use for a specific task is affected by factors not discussed in this report. These factors include the amplitude of the input pulse, the receiver sensitivity, the noise level at the input to the receiver, the clutter level (clutter is a term used for a set of reflections from unwanted "targets" such as ground inhomogeneities) and the frequency range over which data is wanted. Consequently it is not possible to give complete radar design examples in this report: these will be given in a later report in which the system design will be discussed. However, given a specific range and specific values for the ground constitutive parameters, the design chart presented in Figure 6 is an overriding restriction on the use of the HFW.

In order to demonstrate the value of and the use of the data presented in this report, we will assume that we have a 10,000 volt (+80 dB above 1 volt) pulse generator of variable duration, and a receiver which can measure signals to 10 mv in amplitude (-40 dB). We will assume that all noise and clutter signals (in the appropriate range window) are significantly smaller than 10 mv. Let us assume that we have a gauge of the ground conductivity and dielectric constant, and these are approximately σ=0.003 mhos/m and ε_r=9. We wish to detect and/or identify a tunnel whose principal dimensions are of the order of 2m so that its fundamental resonance is about 50 MHz (assuming a lossless target with ε_r=1). First, Figure 6 shows that an HFW radar is feasible if the target is buried 15 m or less.

First, assume a 15 m deep target. We can operate in the HFW, and following Section 8 we choose an antenna length which resonates at approximately 50 MHz, which corresponds to a principal resonance of our target. Figure 1 shows that we will be operating in a region where α is independent of frequency, and a dipole 1 m long will resonate at 50 MHz when ε_r=9. We will assume that a simple dipole matched to a 200 source will be used for both transmitting and receiving, and a "tailored" gaussian doublet (Equation (34)) will be used. Hence, from Table 1, A_1 (see Equation (29) is estimated to be 30 dB. From Table 3 and Figure 26, A_F for d=15 m is estimated to be 80 dB so that the attenuation factor A is about 110 dB. The interface gain of 6 dB on receive reduces A to 104 dB. The difference between the transmitted pulse amplitude and the receiver sensitivity is 120 dB, so that our hypothetical HFW radar can measure the reflections from targets whose reflection introduces an additonal 16 dB attenuation. This reflection loss is typical of results that have been calculated for a tunnel and will be discussed in a future report.

Suppose the target is buried 50 m deep so that Figure 6 determines that an LFW radar must be used. From Figure 20 (or Equation (27)) A is 94 dB if we choose a 20 m dipole. This is modified to 88 dB when the interface gain of 6 dB or receive is included. Next, we calculate the LFW cutoff frequency, from Equation (11), to be 125 KHz. The

received signal will contain significant energy up to this frequency. To obtain a clear range window we transmit a pulse having significant energy up to 10 times this number, or 1.25 MHz, so that the pulse duration should be a little less than 1 μs. The attenuation factor is increased by 15 dB to 103 dB to account for the extra loss introduced by the low pass filtering action of the medium. Thus the radar will detect targets whose reflection coefficients are about -17 dB, but the received signal will contain significant energy in the range zero to 125 KHz as compared to the HFW radar which would receive a signal with a bandwidth of about 40 MHz centered at 50 MHz. However the above quoted calculations of fields scattered by the tunnel give an additional attenuation of the order of 70 dB. Inserting a wire in this tunnel reduces the attenuation to approximately 12 dB in this frequency range. This will also be discussed in a future report.

CONCLUSIONS

The fundamental principles of signal propagation from antennas into lossy media have been examined with a viewpoint on video pulse subsurface radar, and it is concluded that two radar types are required for general subsurface exploration. These are the Low Frequency Window (LFW) radar and the High Frequency Window (HFW) radar. The choice is based on three factors:

1) required depth of operation
2) medium conductivity
3) medium dielectric constant.

HFW radars are suitable for shallow depths and LFW radars must be used for deep and intermediate ranges. A simple design chart has been prepared (Figure 6) so that the radar type applicable to a particular situation can be quickly determined. This chart applies to all electromagnetic subsurface radar systems. It is noted that many pulse type electromagnetic subsurface radar techniques existing at this time operate in the HFW and their range of usefulness is given by the design chart.

Different radar designs are required for the two radar types. For an LFW radar the simple electric dipole in conducting contact with the ground gives a broadband impedance match (down to zero frequency) and practically no signal distortion of a video input pulse can be attributed to the medium or the antenna. Further, signal loss is practically independent of the ground parameters providing the LFW boundary is not exceeded, so that rough estimates of the ground are sufficient to determine accurately the propagation losses. It is emphasized that insulated antennas cannot be used for LFW radars. Basic attenuation curves obtained using a gaussian pulse have been presented, and these curves are applicable to any signal providing its frequency spectrum falls within the LFW.

For an HFW radar it makes little difference whether the antenna is bare or insulated: insulated antennas have the advantage of being readily portable. In the HFW propagation is effectively similar to free space propagation with the addition of an exponential attenuation factor. The antenna length, and pulse type and duration must be "tailored" to the application of the radar for most effective operation. Basic attenuation curves have been presented for a variety of parameters pertinent to tunnel detection.

This report has focussed attention on the fundamental propagation factors associated with subsurface radar systems. A forthcoming report will deal further with introducing the scattering from cylindrical geometries into this basic model. In addition attention will be focused on more sophisiticated antennas with a view toward optimizing the detectability task. Further attention is being focused on the target identification task.

REFERENCES

Bates, R. H. T., 1967, "Comments on Radiating Elements which would have good transient responses", unpublished note.

Bates, R. H. T., and Burrell, G. A., 1972, "Towards faithful radio transmission of very wide bandwidth signals", IEEE Trans., v. AP-20, pp. 684-690.

Bergland, G. D., 1969, "A guided tour of the fast Fourier transform", IEEE Spectrum, v. 6, n. 7, pp. 41-52.

Burrell, G. A., 1971, "Transients in antennas", Christchurch, Ph.D. Thesis, University of Canterbury, New Zealand.

Burrell, G. A., 1972, "Experimental determination of the input impedance of an effectively infinite monopole", Proc. IREE (Australia), v. 33, pp. 393-394.

Burrell, G. A., and Munk, B. A., 1976, "The array scanning method and applying it to determine the impedance of linear antennas in a lossy half space", Report 4460-1, October 1976, The Ohio State University ElectroScience Laboratory, Department of Electrical Engineering; prepared under Contract DAAG53-76-C-0179 for U. S. Army Mobility Equipment Research and Development Command.

Burrell, G. A. and Peters, L., Jr., 1976, "Design of electromagnetic pulse (EMP) radars for geological exploration at depths of several kilometers", Report, ElectroScience Laboratory, The Ohio State University, 25 February.

Collin, R. E. and Zucker, F. J. (Eds.), 1969, Antenna Theory, part II, New York, McGraw-Hill.

Dion, A. R., "Transmission of step functions by loop antennas", IEEE Trans., v. AP-18, pp. 389-392.

Gabillard, R., Degauque, P., and Wait, J. R., 1971, "Subsurface Electromagnetic telecommunication - a review", IEEE Trans. on Communication Technology, v. COM-19, pp. 1217-1228.

Lager, D. L. and Lytle, R. J., 1975, "Fortran subroutines for the numerical evaluation of Sommerfeld integrals unter anderem", Lawrence Livermore Laboratory Report UCRL-51821, May 21.

Lerner, R. M., 1974, Ground radar system, U.S. Patent 3,831,173, August 20.

Melton, B. S., 1937, Electromagnetic prospecting method, U.S. Patent 2,077,707, April 20.

Moffatt, D. L. and Mains, R. K,. 1975, "Detection and Discrimination of Radar Targets", IEEE Trans., v. AP-23, pp. 358-367.

Moffatt, D. L., Puskar, R. J. and Peters, L., Jr., 1973, "Electromagnetic pulse sounding for geological surveying with application in rock mechanics and the rapid excavation program," Report 3408-2, The Ohio State University ElectroScience Laboratory, Department of Electrical Engineering; prepared under Contract H0230009 for Advanced Research Projects Agency.

Richmond, J. H., 1974a, "Computer program for thin-wire structures in a homogeneous conducting medium", Report NASA-CR-2399.

---- , 1974b, "Radiation and scattering by thin-wire structures in a homogeneous conducting meidum", IEEE Trans., v. AP-22, p. 365.

Ross, G. F., 1965, "The synthetic generation of phase coherent microwave signals for transient behavior measurements", IEEE Trans., v. MTT-13, pp. 704-706.

Ross, G. F., 1967, "A new wideband antenna receiving element", IEEE NEREM Record, pp. 78-79.

Schelkunoff, S. A., and Friis, H. T., 1952, Antennas, theory and practice, New York, John Wiley.

Young, J. D., 1975, "A transient underground radar for buried pipe location", 1975 USNC/URSI Meeting, Boulder, Colo., October 23.

Young, J. D. and Caldecott, R., 1976, Underground pipe detector, U. S. Patent 3,967,282, June 29.